Non-hydrostatic Atmospheric GCM Development and its Computational Performance

K.Takahashi, X.Peng, K.Komine, M.Ohdaira, Y.Abe, T.Sugimura, K.Goto, H.Fuchigami, M.Yamada

Earth Simulator Center, JAMSTEC

Contents

- Motivation & Targets
- Developing Strategy
  - Grid System
  - Differential schemes for time/space
- Preliminary Validation Results
  - Atmosphere & Ocean
- Simulation for non-hydrostatic phenomena
- High Performance Computation on the ES
- Near Future Work

Climate System

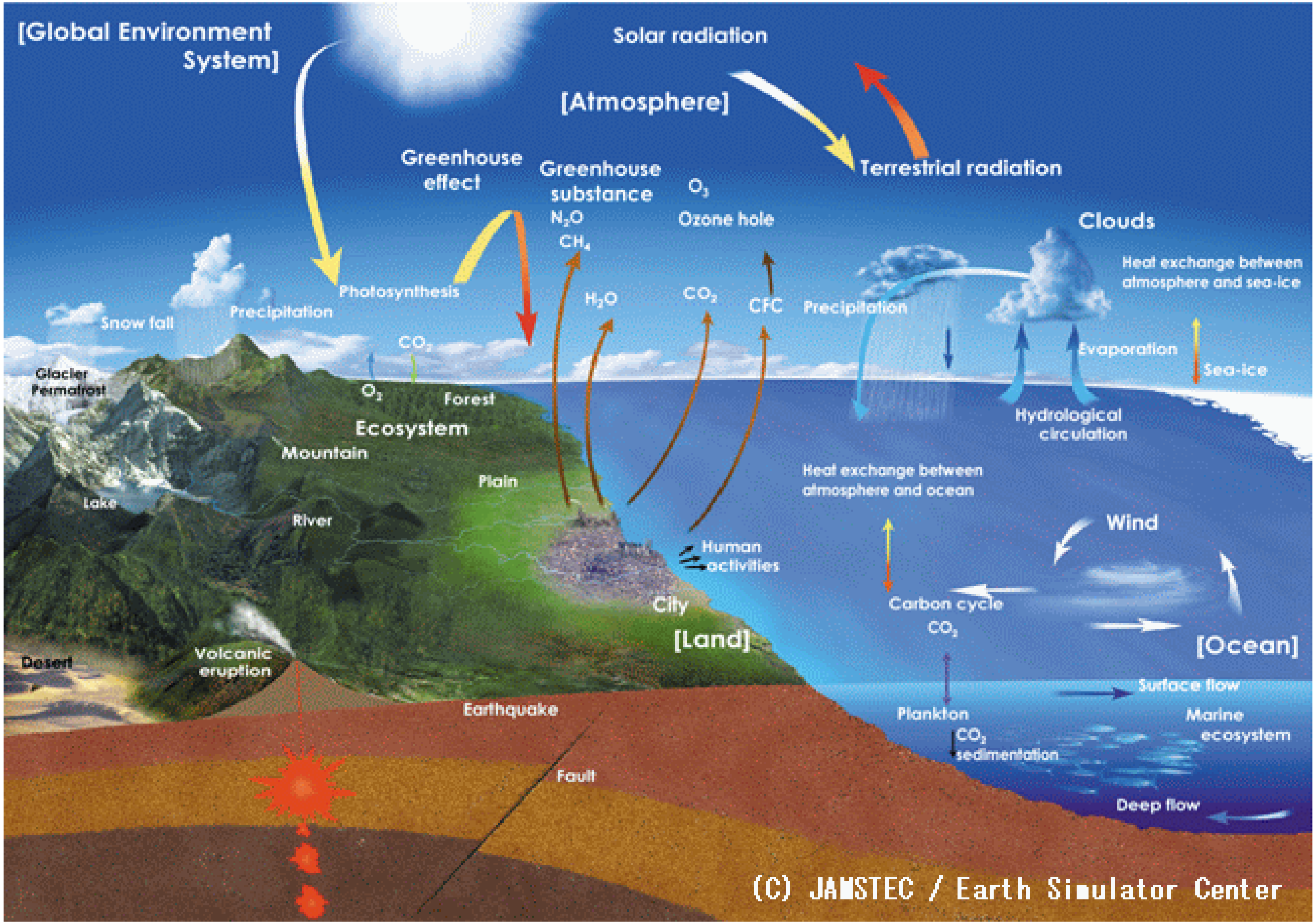

Time/Space scale

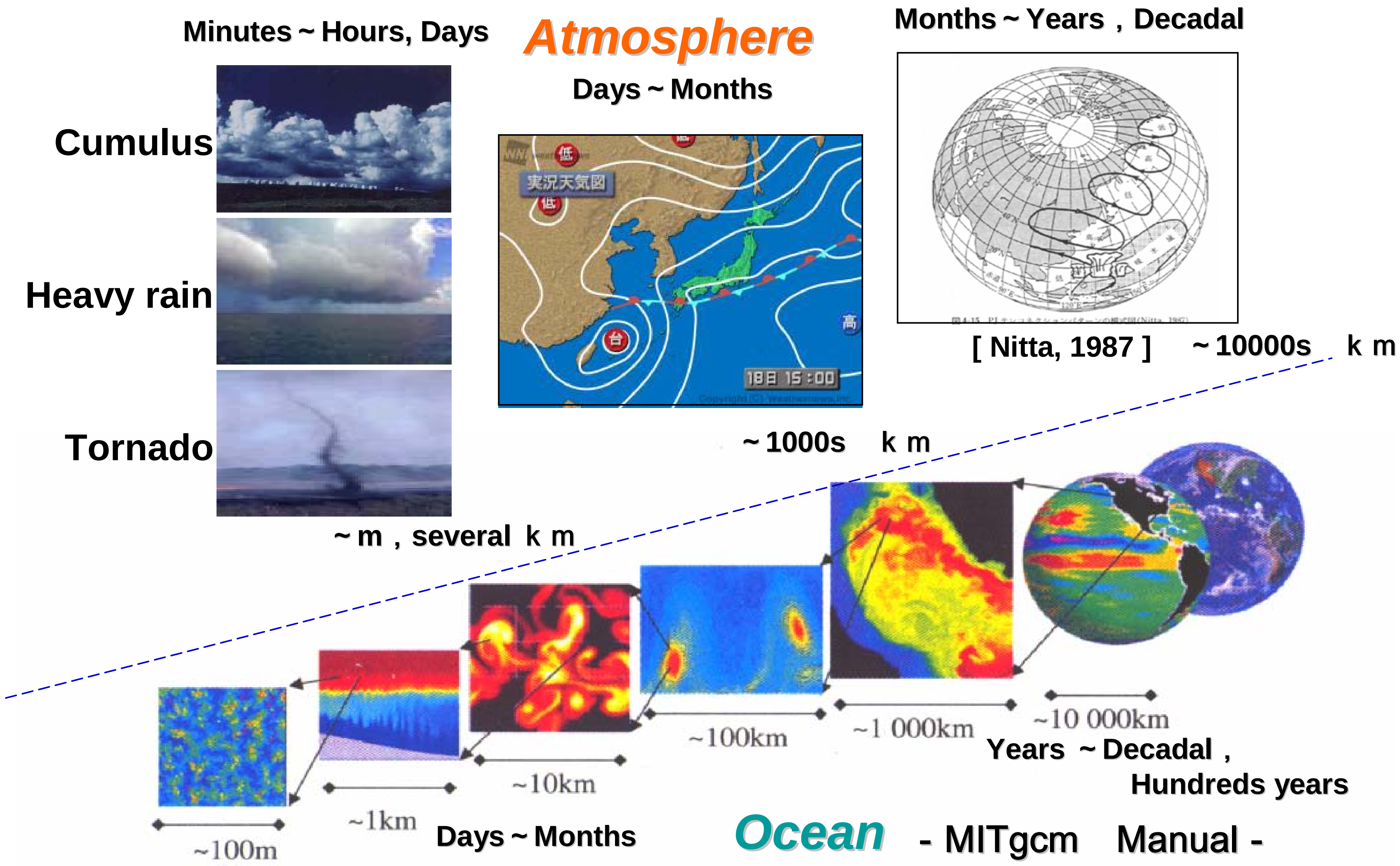

Front system

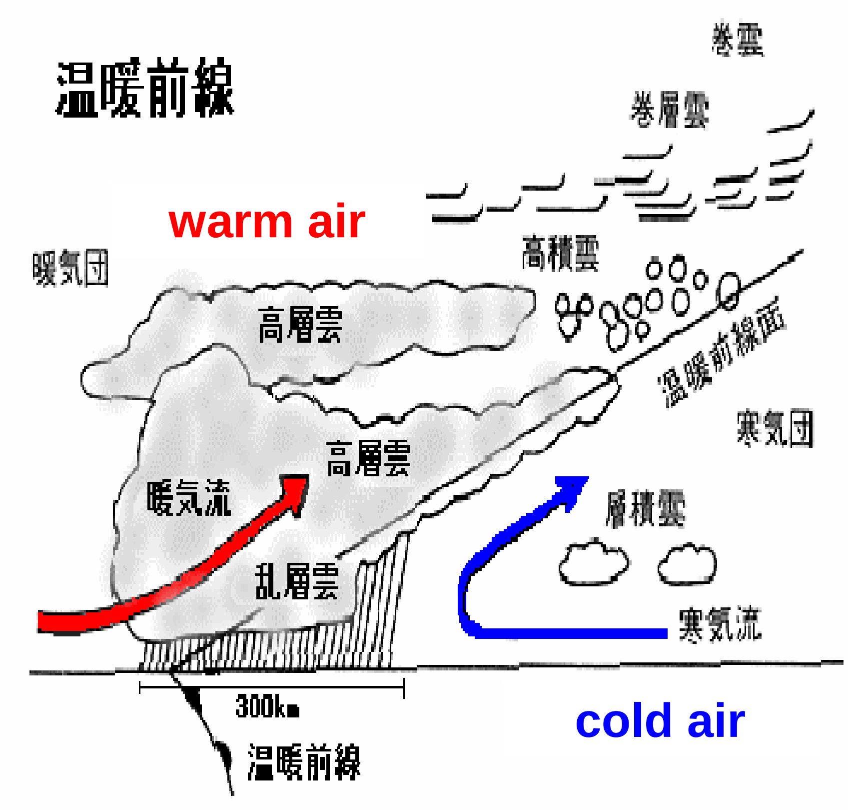

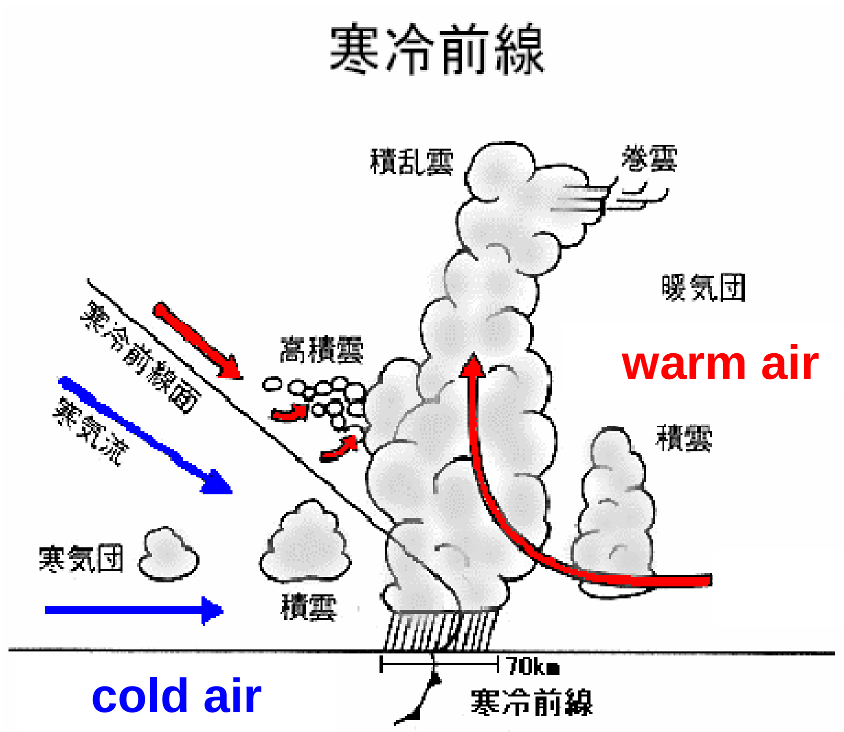

Cloud System

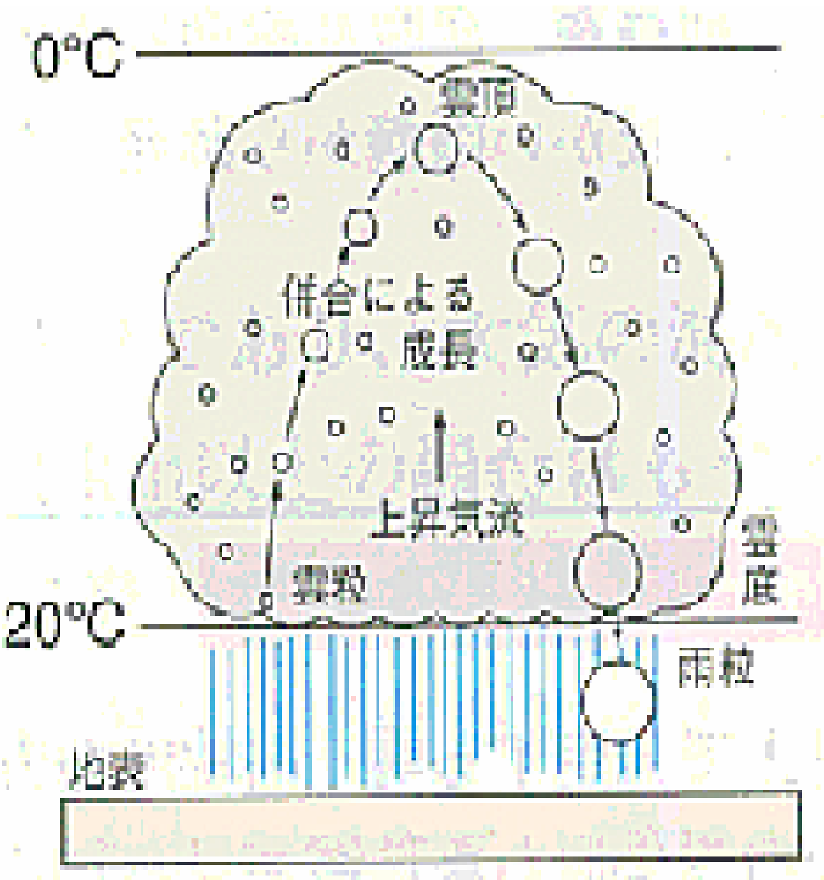

← O(100)m ~ O(1)km →

Warm Rain

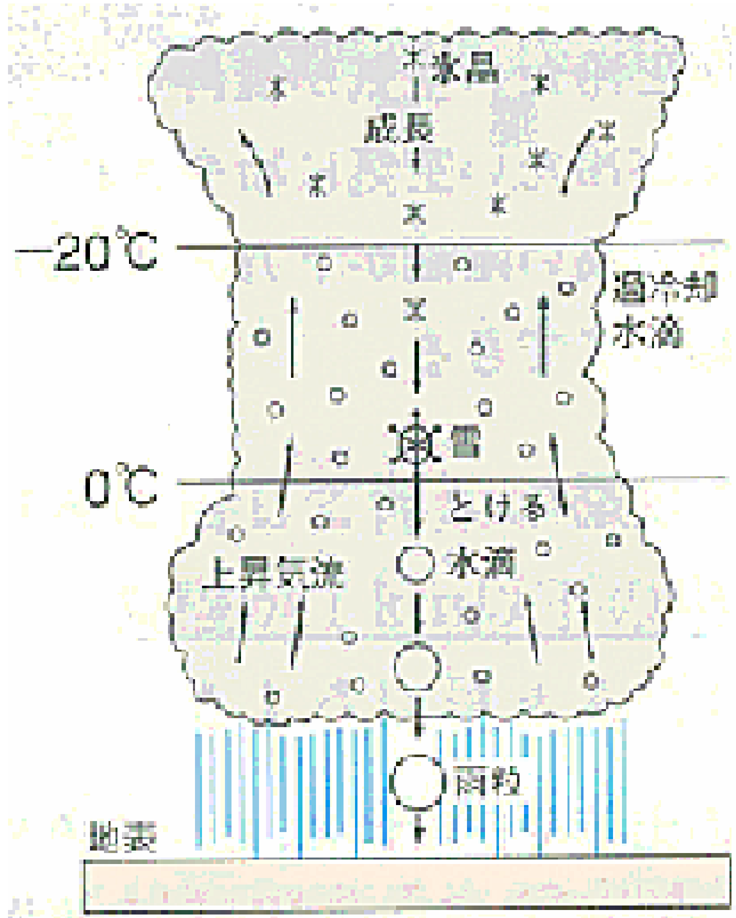

← O(100)m ~ O(1)km →

Cold Rain

Grid System

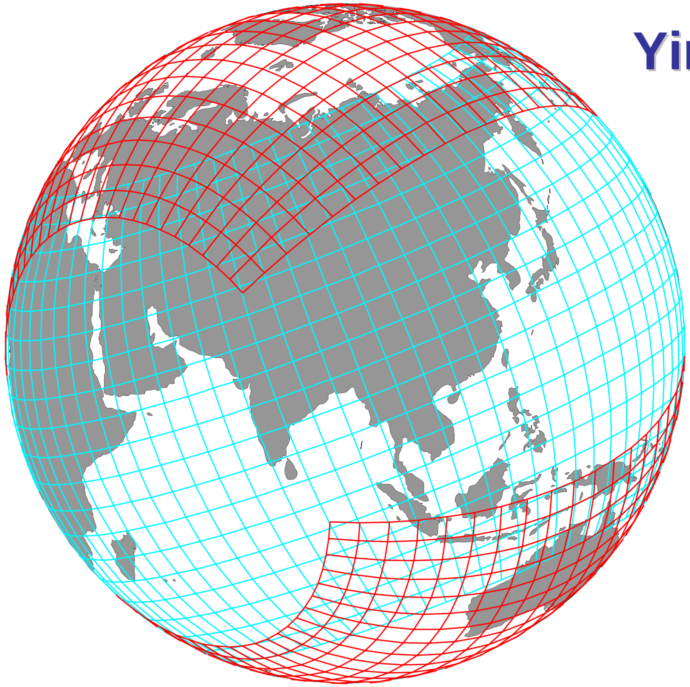

Yin-Yang Grid System

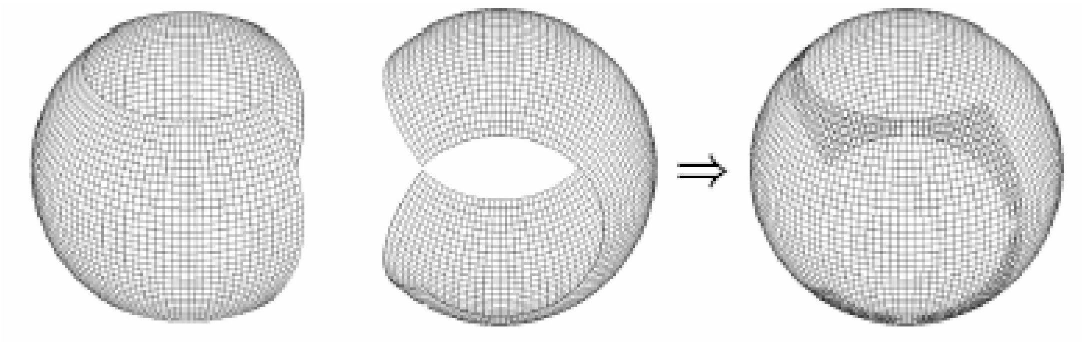

New Reduced Grid System

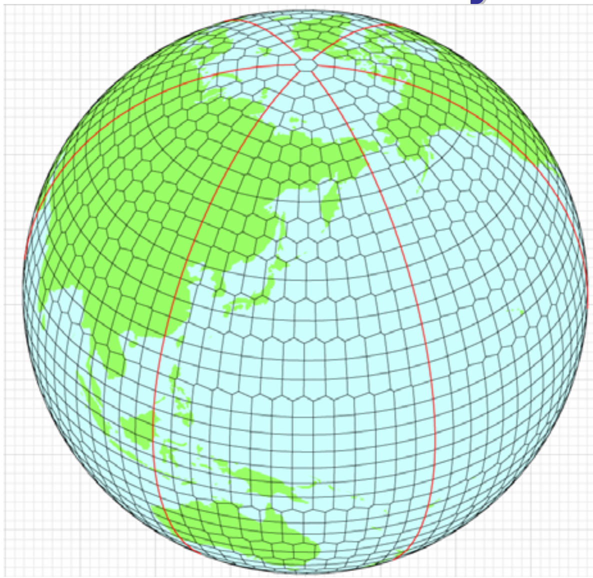

- **Orthogonal coordinates.**
  (same as the lat-lon geometry)
- **No polar singularity.**
- **Relax of CFL condition.**
- **The same grid structure of N and E component.**
- **Easy to nest.**
- **High parallelization.**
- **But need to take care of conservation law.**

Continuity equation

$$\frac{\partial\rho}{\partial t} = -\frac{1}{a\cos\varphi}\left(\frac{\partial(\rho U)}{\partial\lambda} + \frac{\partial(\cos\varphi\rho V)}{\partial\varphi}\right) - \frac{1}{a^2}\frac{\partial(a^2\rho W^*)}{\partial z^*}$$

Momentum equation

$$\begin{aligned}\frac{\partial(\rho U)}{\partial t} &= -\frac{1}{a\cos\varphi}\left(\frac{\partial(\rho UU)}{\partial\lambda} + \frac{\partial(\cos\varphi\rho UV)}{\partial\varphi}\right) - \frac{1}{a^2}\frac{\partial(a^2\rho UW^*)}{\partial z^*}\\ &- \frac{1}{a\cos\varphi}\frac{\partial P}{\partial\lambda} - \frac{G^{\frac{1}{2}}G^{13}}{G^{\frac{1}{2}}a\cos\varphi}\frac{\partial P}{\partial z^*} + 2\Omega_r\rho V - 2\Omega_\varphi\rho W + \frac{\rho UV\tan\varphi}{a} - \frac{\rho UW}{a} + F_\lambda\end{aligned}$$

$$\begin{aligned}\frac{\partial(\rho V)}{\partial t} &= -\frac{1}{a\cos\varphi}\left(\frac{\partial(\rho UV)}{\partial\lambda} + \frac{\partial(\cos\varphi\rho VV)}{\partial\varphi}\right) - \frac{1}{a^2}\frac{\partial(a^2\rho VW^*)}{\partial z^*}\\ &- \frac{1}{a}\frac{\partial P}{\partial\varphi} - \frac{G^{\frac{1}{2}}G^{23}}{G^{\frac{1}{2}}a}\frac{\partial P}{\partial z^*} + 2\Omega_\lambda\rho W - 2\Omega_r\rho U - \frac{\rho UU\tan\varphi}{a} - \frac{\rho VW}{a} + F_\varphi\end{aligned}$$

$$\boxed{\begin{aligned}\frac{\partial(\rho W)}{\partial t} &= -\frac{1}{a\cos\varphi}\left(\frac{\partial(\rho UW)}{\partial\lambda} + \frac{\partial(\cos\varphi\rho VW)}{\partial\varphi}\right) - \frac{1}{a^2}\frac{\partial(a^2\rho WW)}{\partial z^*}\\ &- \frac{1}{G^{\frac{1}{2}}}\frac{\partial P}{\partial z^*} - \rho\boldsymbol{g} + 2\Omega_\varphi\rho U - 2\Omega_\lambda\rho V + \left(\frac{\rho UU}{a} + \frac{\rho VV}{a}\right) + F_r\end{aligned}}$$

Pressure equation

$$
\begin{aligned}
\frac{\partial P}{\partial t} = \\
- & \left(\frac{1}{a\cos\varphi}\frac{\partial PU}{\partial\lambda} + \frac{1}{a\cos\varphi}\frac{\partial PV\cos\varphi}{\partial\varphi} + \frac{1}{a^2}\frac{\partial a^2 PW^*}{\partial z^*} \right) \\
- & (\gamma - 1)P \left(\frac{1}{a\cos\varphi}\left(\frac{\partial U}{\partial\lambda} + \frac{\partial(\cos\varphi V)}{\partial\varphi} \right) + \frac{1}{a^2}\frac{\partial(a^2 W^*)}{\partial z^*} \right) \\
+ & (\gamma - 1)K \frac{1}{a^2 G^{\frac{1}{2}}\cos\varphi} (\\
& + \frac{\partial}{\partial\lambda}\left(\frac{G^{\frac{1}{2}}}{\cos\varphi}\frac{\partial T}{\partial\lambda} \right) + \frac{\partial}{\partial\lambda}\left(\frac{G^{\frac{1}{2}}G^{13}}{\cos\varphi}\frac{\partial T}{\partial z^*} \right) \\
& + \frac{\partial}{\partial\varphi}\left(G^{\frac{1}{2}}\cos\varphi\frac{\partial T}{\partial\varphi} \right) + \frac{\partial}{\partial\lambda}\left(G^{\frac{1}{2}}G^{23}\cos\varphi\frac{\partial T}{\partial z^*} \right) \\
& + \frac{\partial}{\partial z^*}\left(\frac{G^{\frac{1}{2}}G^{13}}{\cos\varphi}\frac{\partial T}{\partial\lambda} \right) + \frac{\partial}{\partial z^*}\left(G^{\frac{1}{2}}G^{23}\cos\varphi\frac{\partial T}{\partial\varphi} \right) + \frac{\partial}{\partial z^*}\left(\frac{a^2\cos^2\varphi + (G^{\frac{1}{2}}G^{23}\cos\varphi)^2 + (G^{\frac{1}{2}}G^{13})^2}{\cos\varphi G^{\frac{1}{2}}}\frac{\partial T}{\partial z^*} \right)) \\
+ & (\gamma - 1)\Phi
\end{aligned}
$$

Equation of state

$$
P = \rho RT
$$

Mass conserving numerical scheme

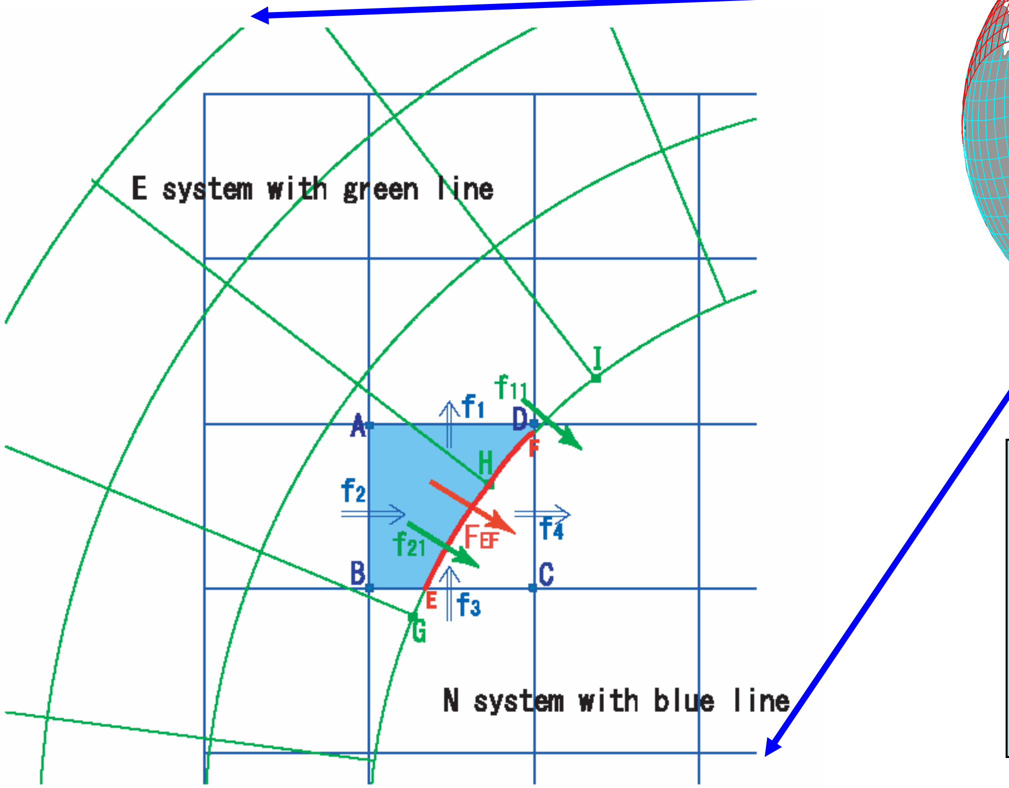

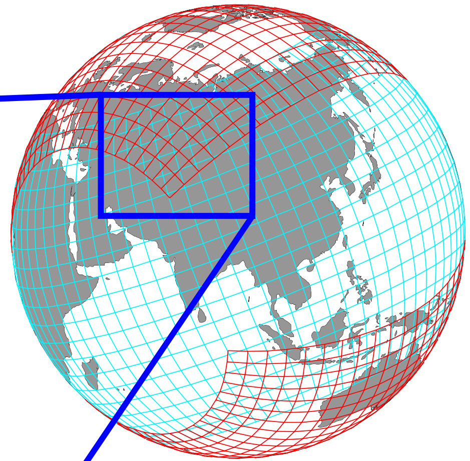

Computation all of fluxes on computational grids

Correction for conserving

For flux F_{EF} on a circular arc EFshown as red circle is computed by the budget of fluxes f_N by on grid ABCD of N system and flux f_E estimated on a circular arc GHI of E system.

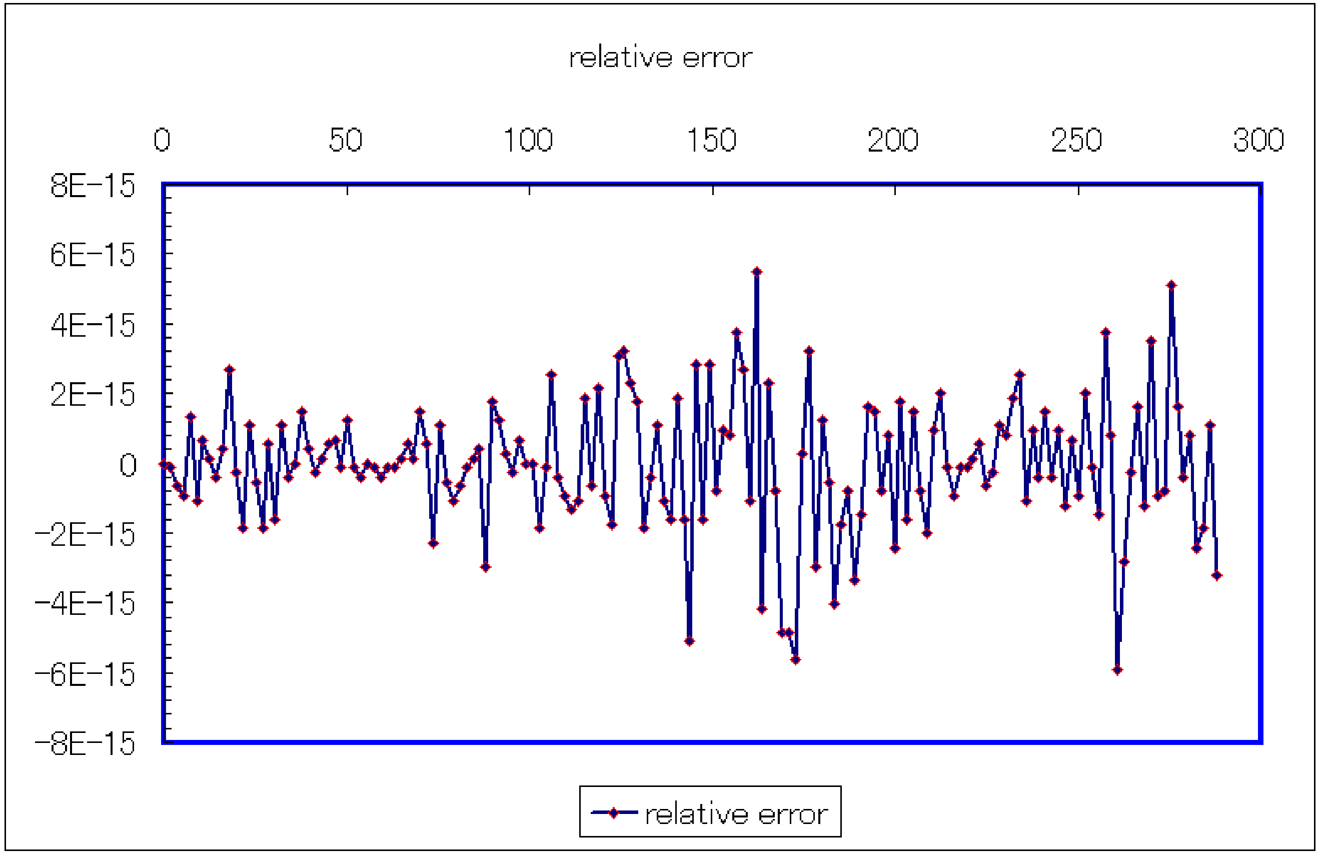

Using this conservative scheme, we have evaluated that time evolution of relative error of the mass has changed within the limit of rounding error.

Numerical sensitivity experiments to shallow water equations

Test Case 1 : Advection of Cosine Bell over the Pole

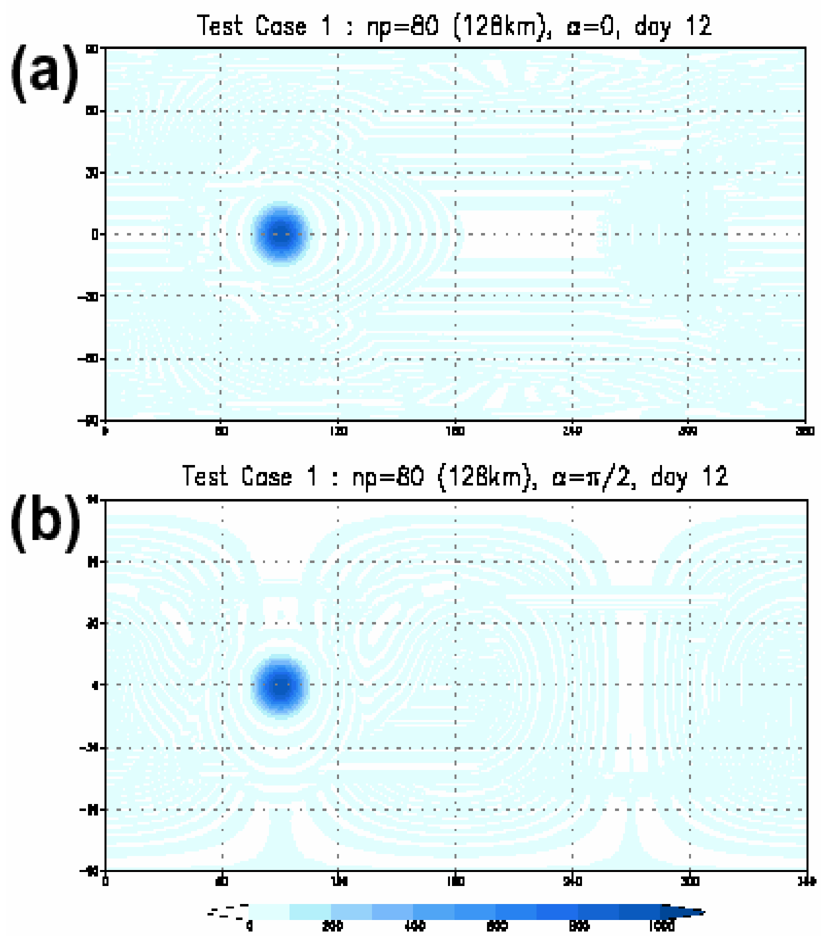

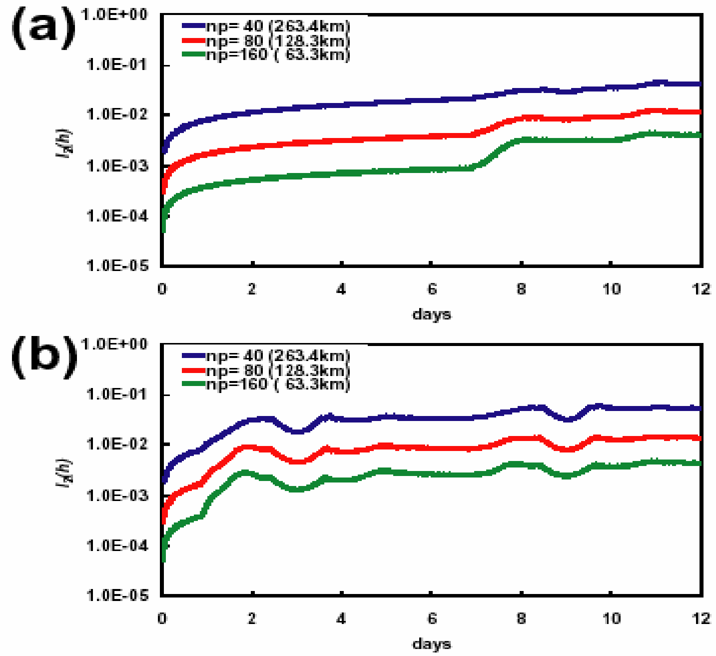

The 2nd-order accuracy is maintained for any horizontal resolution.

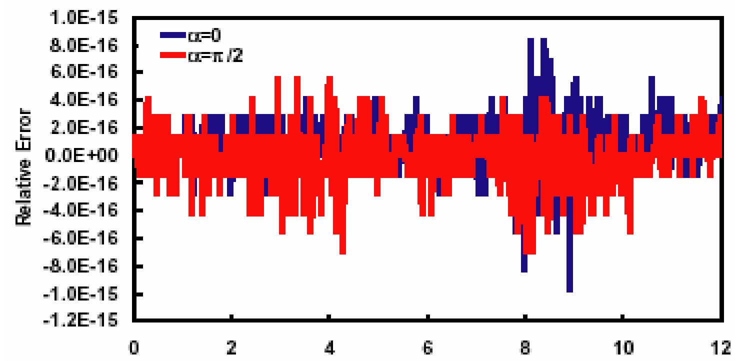

Well mass conserved results

Test Case 2 : Global Steady State
Nonlinear Zonal Geostropic Flow

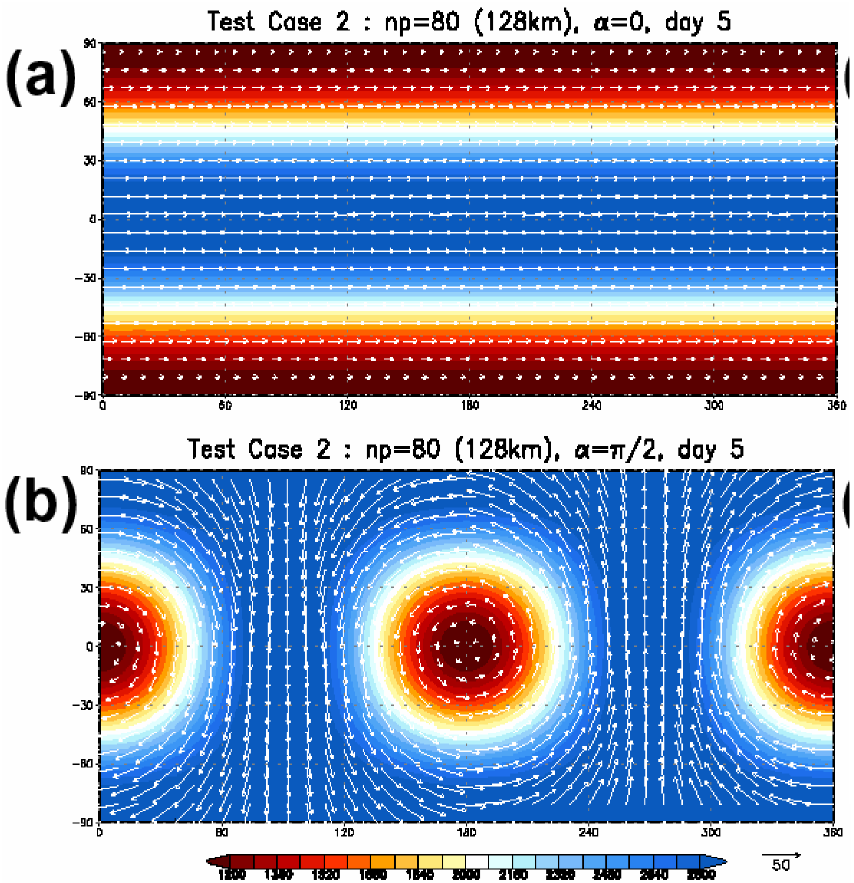

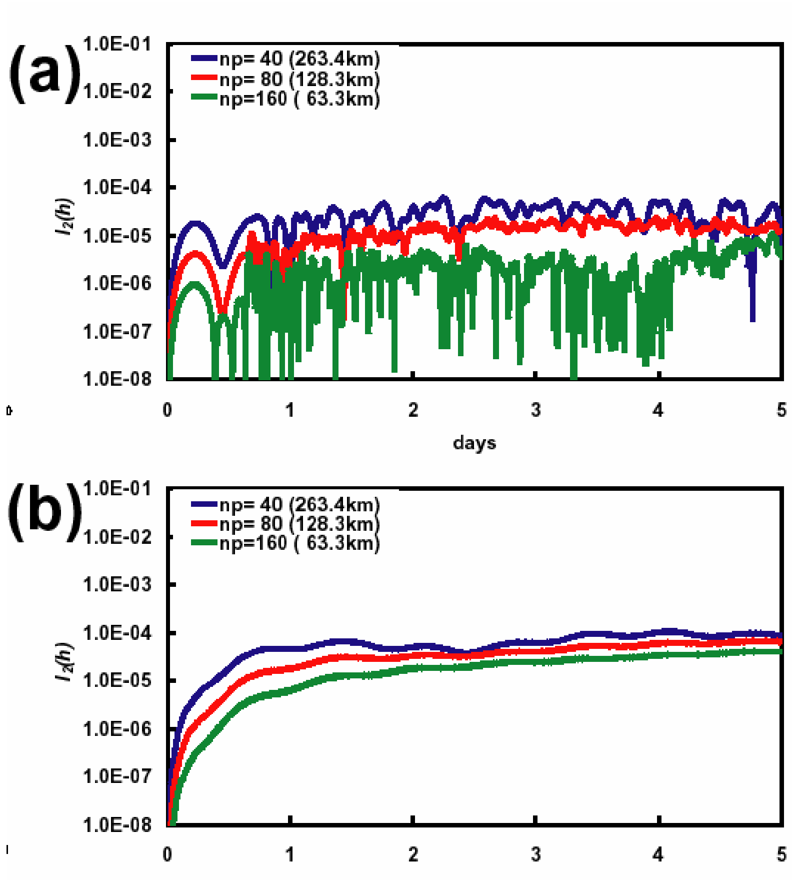

The solid body rotation field is maintained.

The 2nd-orderaccuracy is maintained.

Test Case 5 : Zonal Flow over an Isolated Mountain

Simulation Results

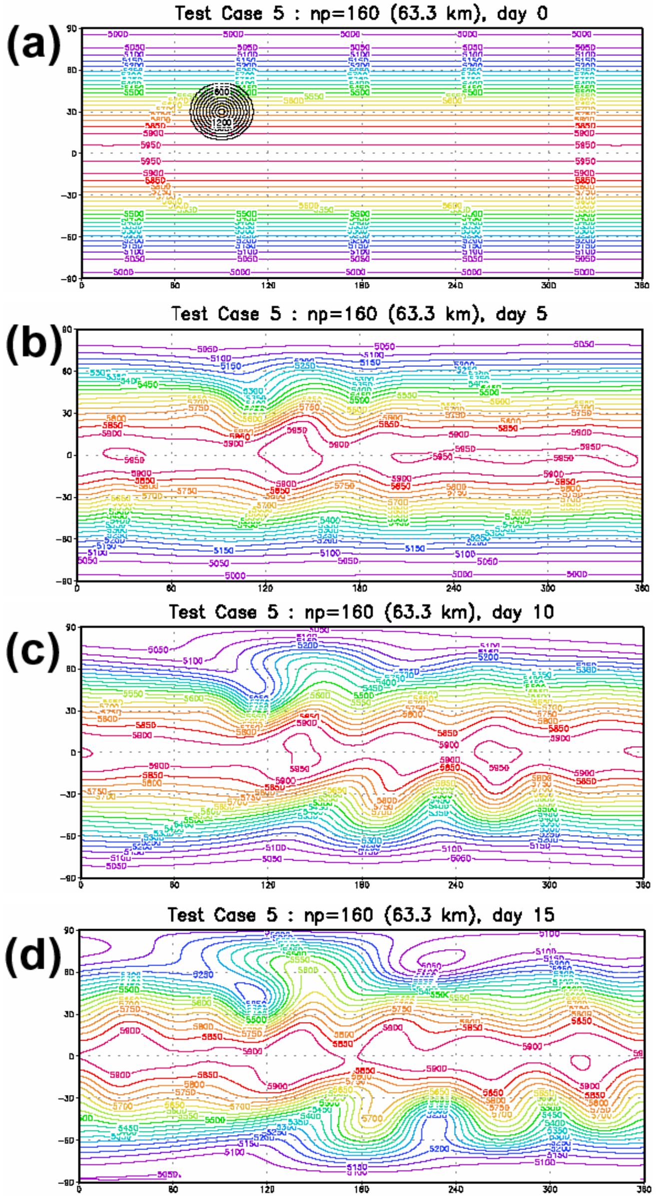

Results with spectral scheme

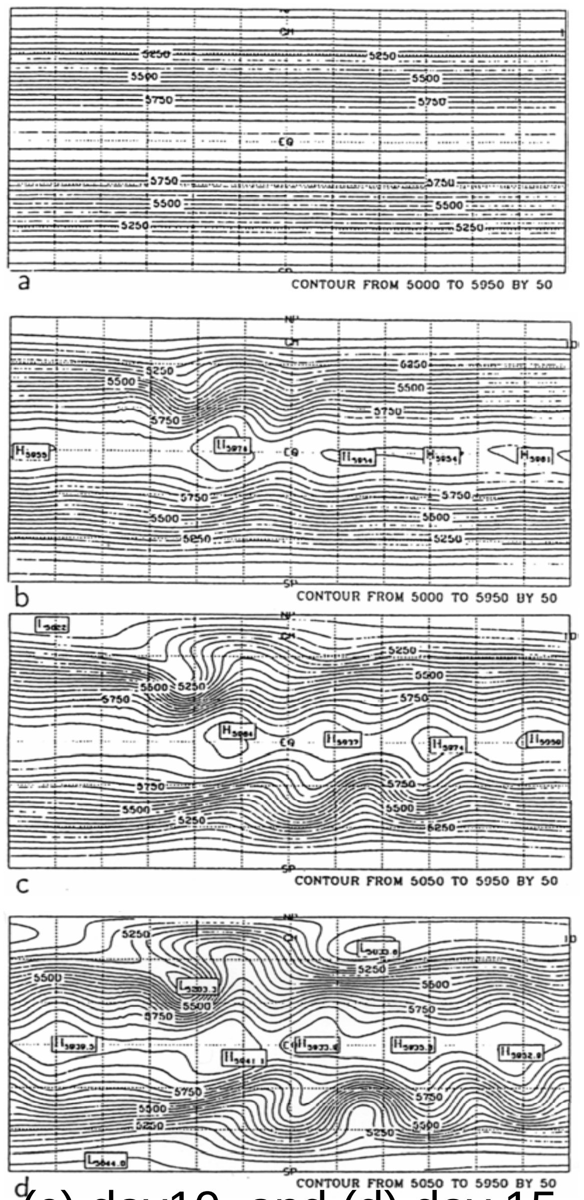

R. Jakob, J. J. Hack and D. L. Williamson, Solutions to the Shallow Water Test Set Using the Spectral Transform Method., NCAR/TN-388+STR, 1993

Field at (a) day 0, (b) day 5, (c) day10, and (d) day 15.

Test Case 6 : Rossby-Haurwitz Wave

Simulation Results **Results with spectral scheme**

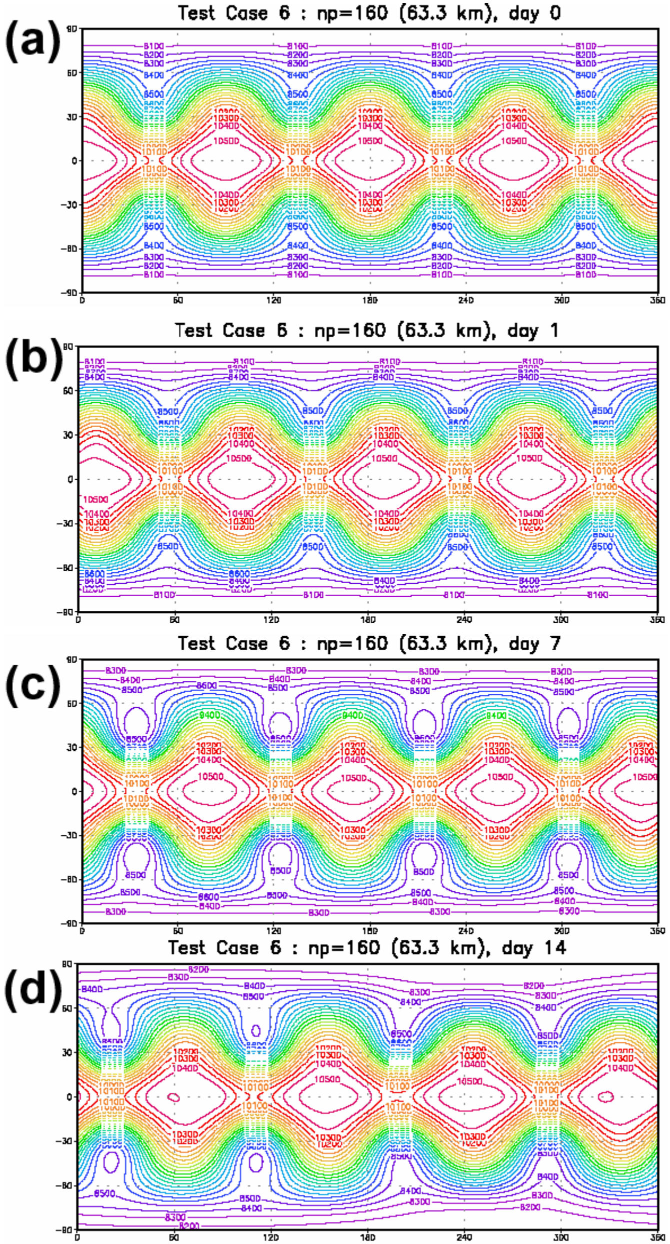

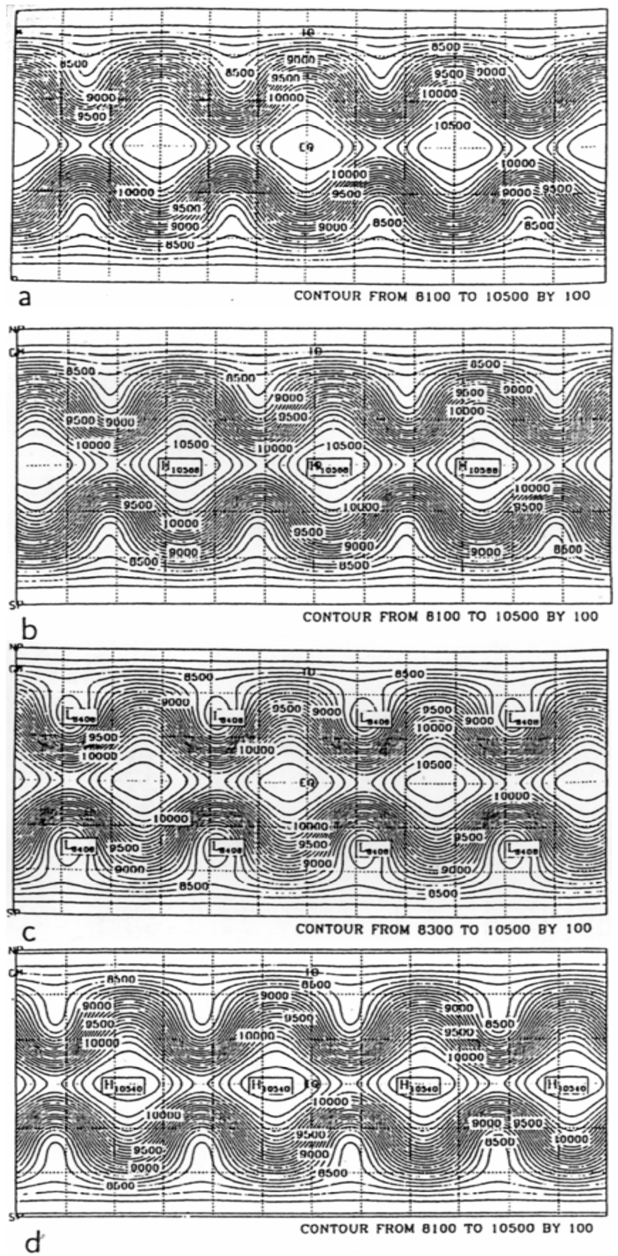

Rossby-Haurwitz wave shape has been propagated from the west to the east without change from initial field after 14 days integration.

R. Jakob, J. J. Hack and D. L. Williamson, Solutions to the Shallow Water Test Set Using the Spectral Transform Method., NCAR/TN-388+STR, 1993

Mountain waves experiments

- The height of the top of the code is 40 km and uses 24 vertical layers equally spaced in z^* .
- We set the mountain height h =1000m and the half-width d =1250km .
- The Brunt-Vaisala frequency is N=0.0187 s^{-1} .
- Set uniform zonal mean easterly flow of $u = -40\cos\varphi$ m s^{-1} .
- Rayleigh damping layer are set from top to 2/3 height for

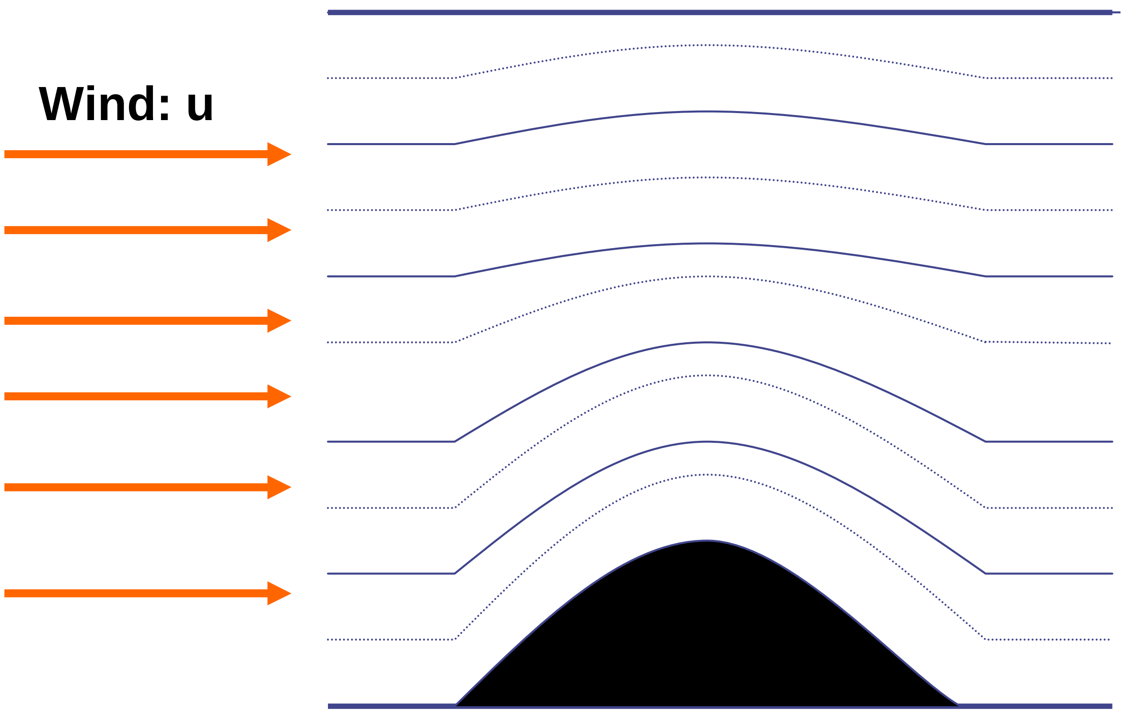

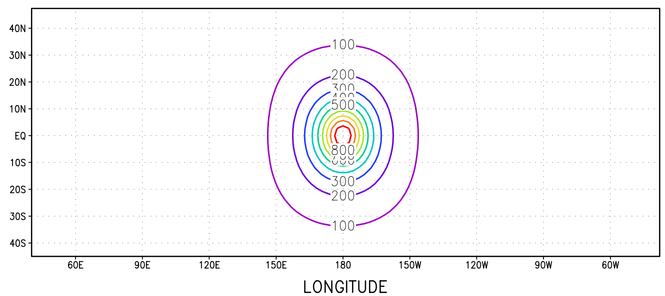

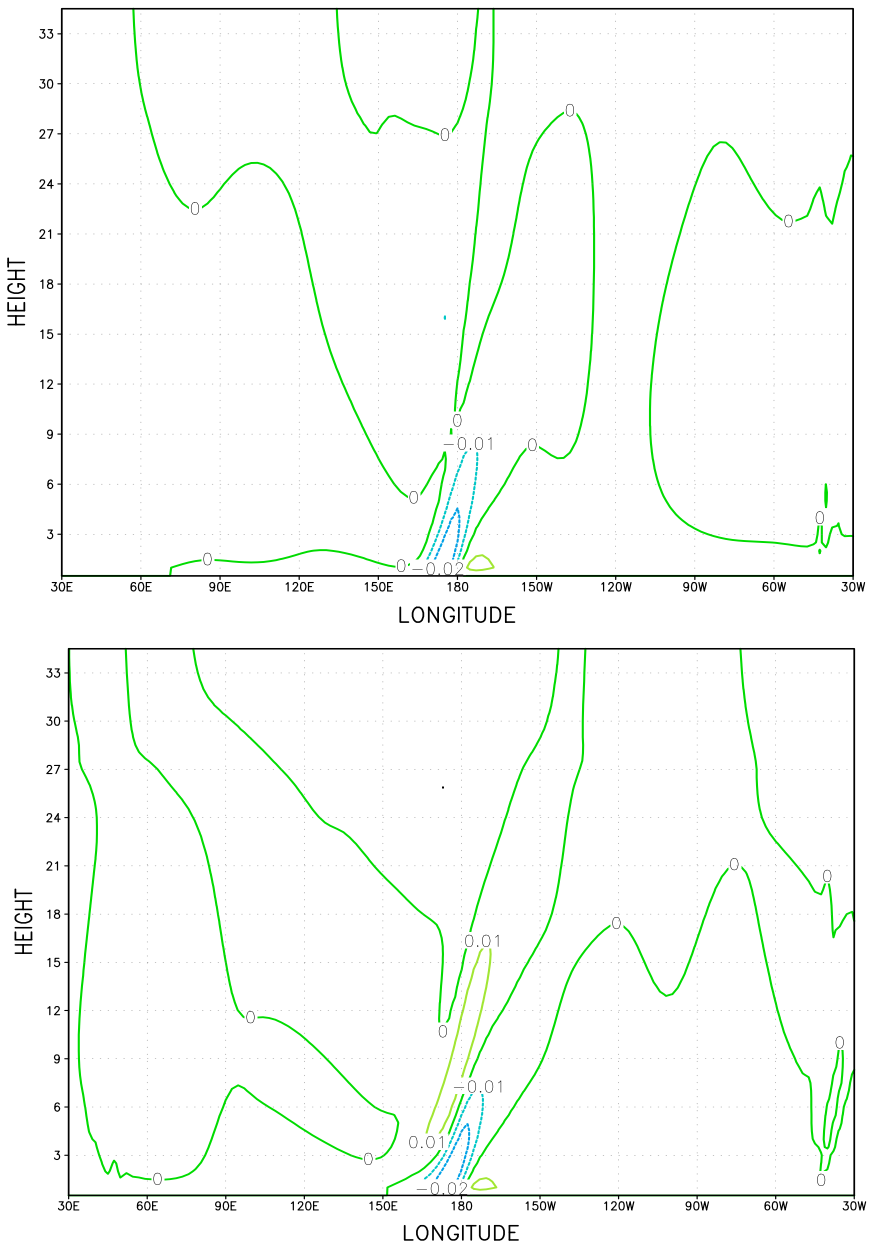

The λ-*z* cross section of vertical wind speed *w* (m s-1) along the equator after 12, 24hours.

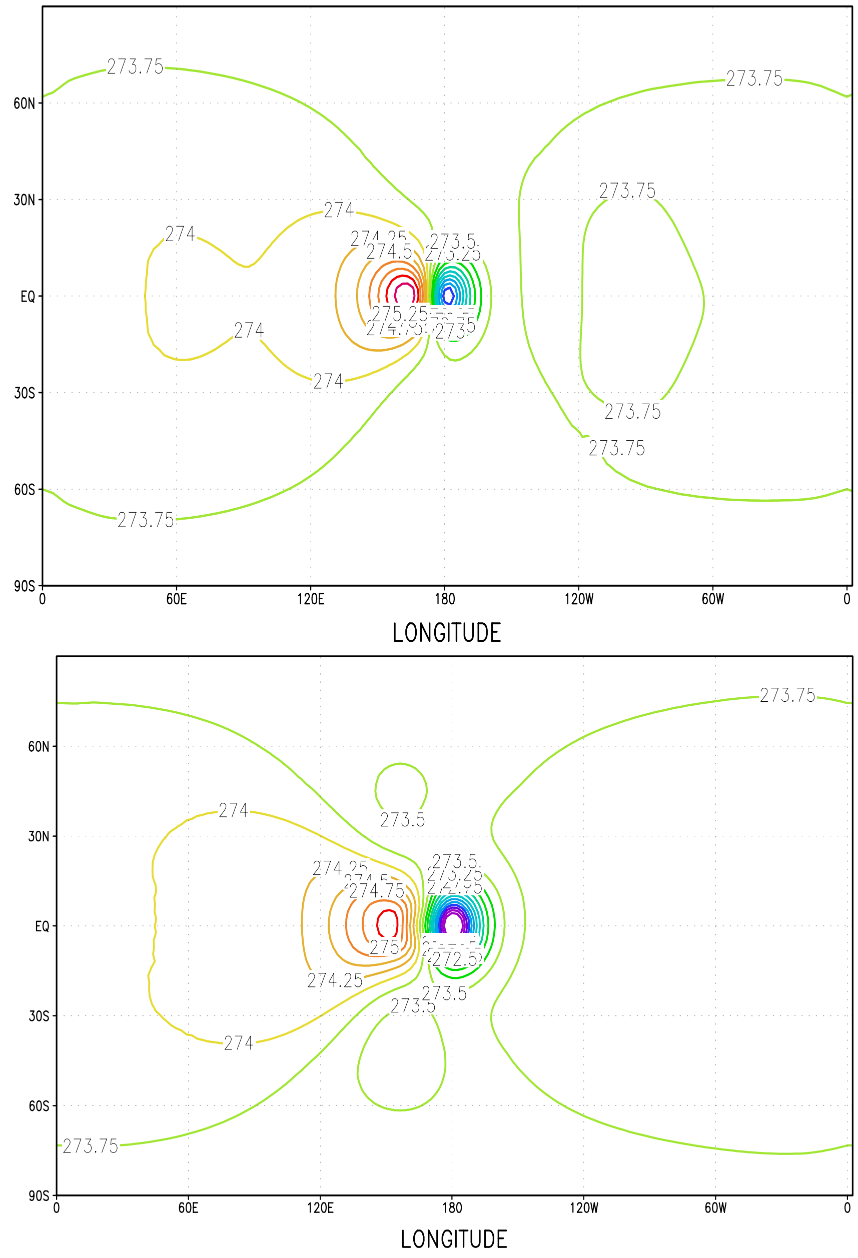

Temperature (K) at 0km (bottom) levels after 12, 24hours.

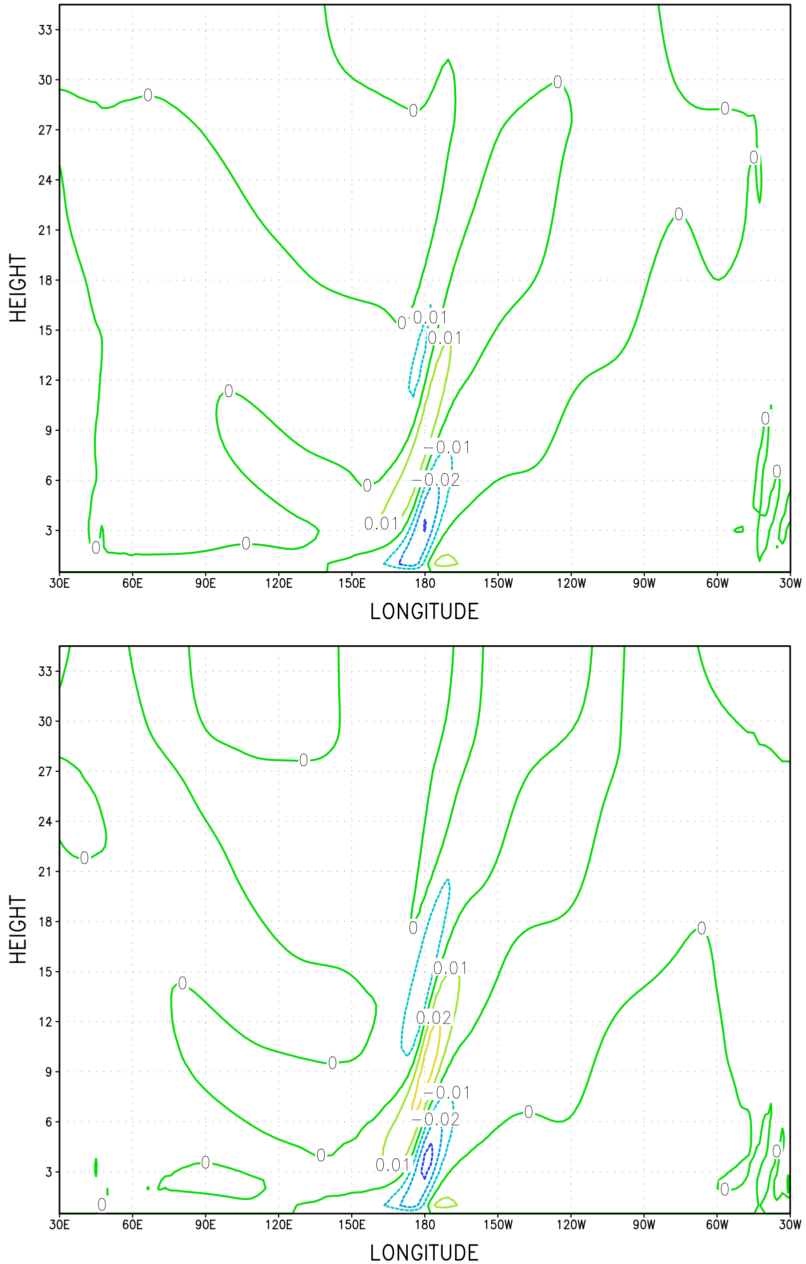

The λ-*z* cross section of vertical wind speed *w* (m s-1) along the equator after 36, 48 hours.

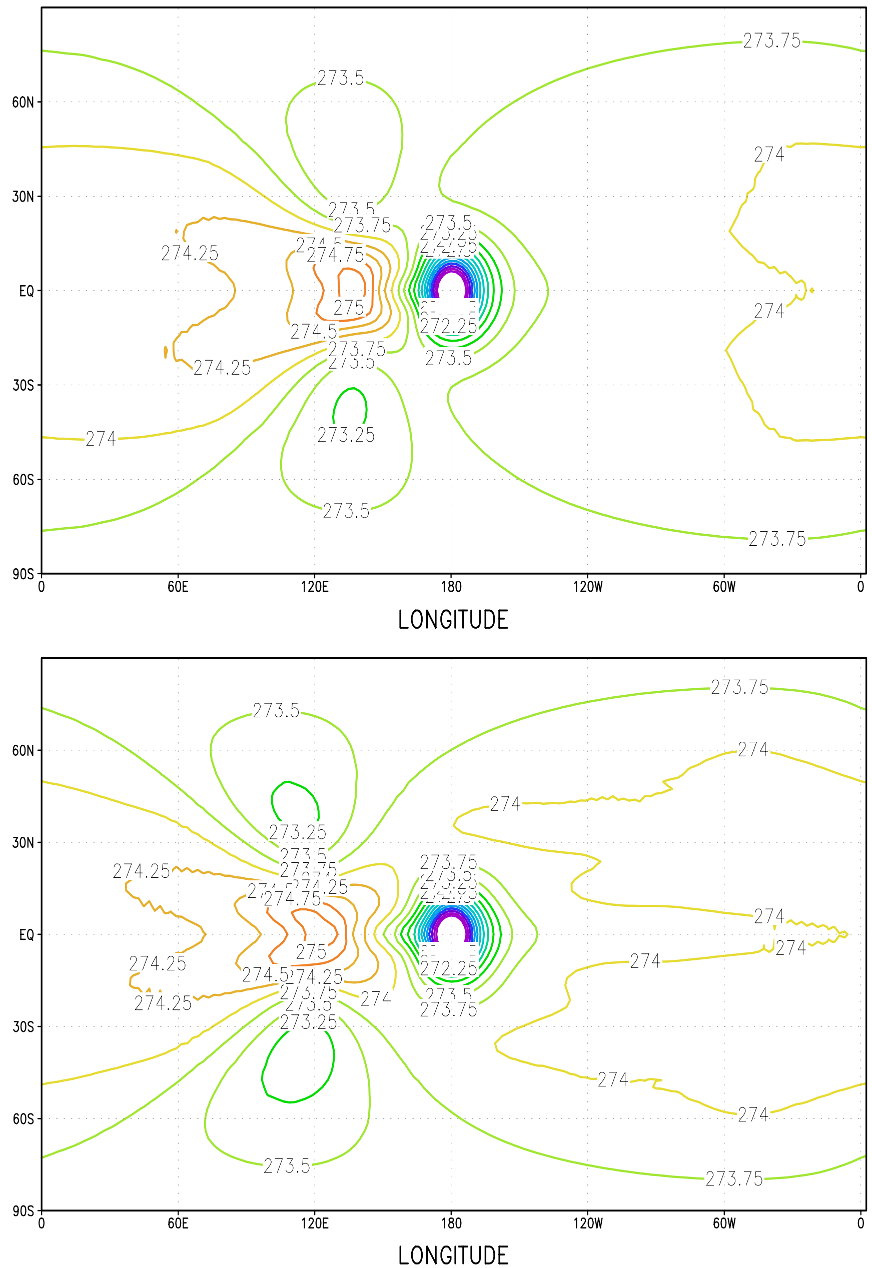

Temperature (K) at 0km (bottom) levels After 36, 48 hours.

Held and Suarez experiment

In order to verify long-term statistical properties of a fully developed general circulation a benchmark calculation proposed by Held and Suarez(1994) were performed.

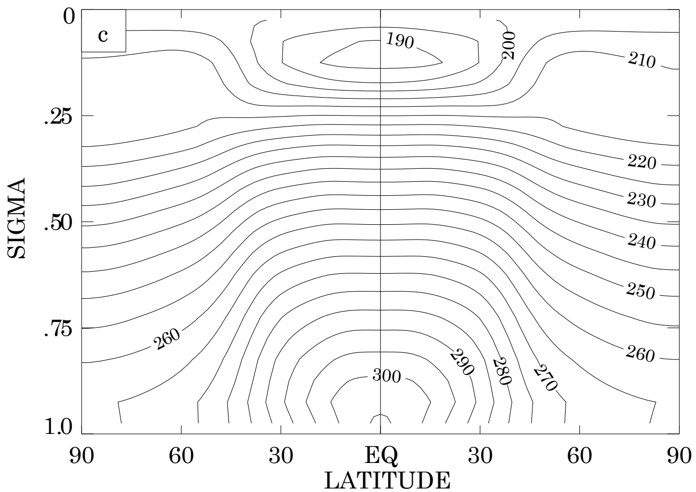

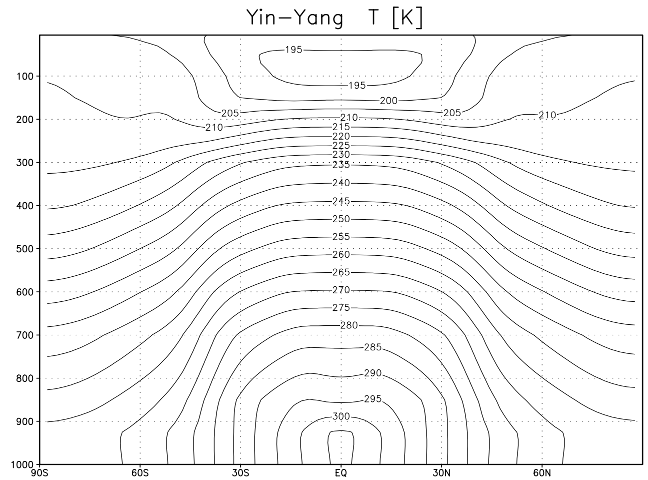

The zonal mean temperature *T* [K] (a) Held and Suarez, (b) Results using Yin-Yang grid.

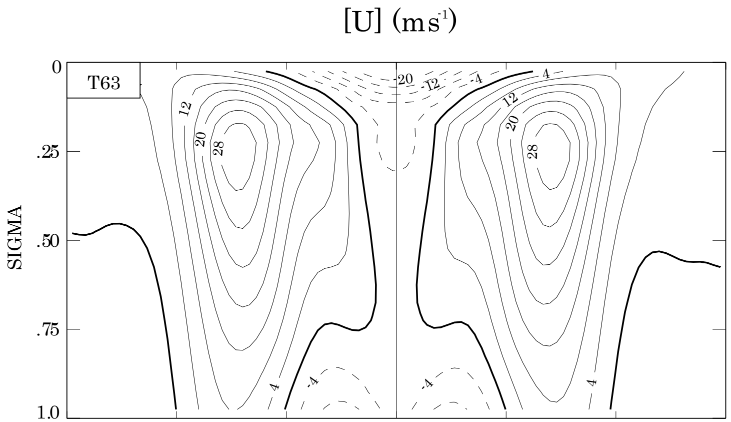

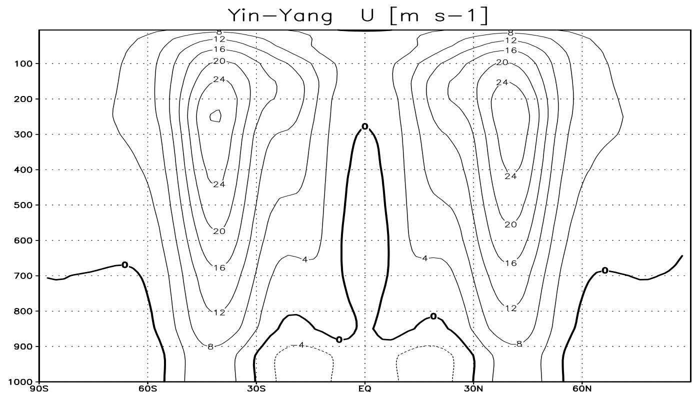

The zonal mean zonal wind *U* [m sec-1] (a) Held and Suarez, (b) Results on Yin-Yang grid.

Vertical differencing of primitive equations

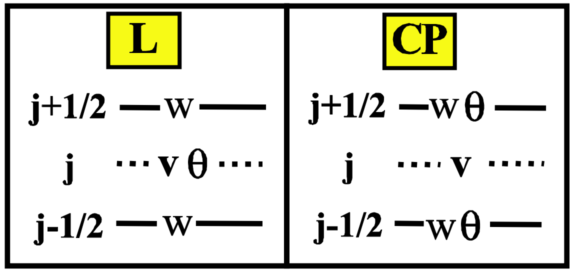

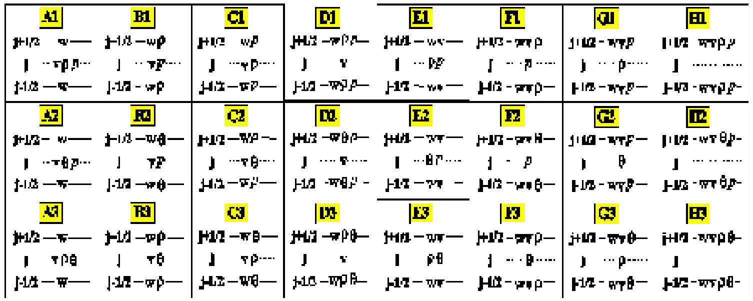

All cases of vertical staggering

24 cases, which are whole combinatorial cases of Lorenz types and Charney-Phillips types vertical staggering, were examined to identify those features. Charney-Phillips type distribution, case B2 in Figure 6, shows best, though it is required to dissipate 2 grid oscillations.

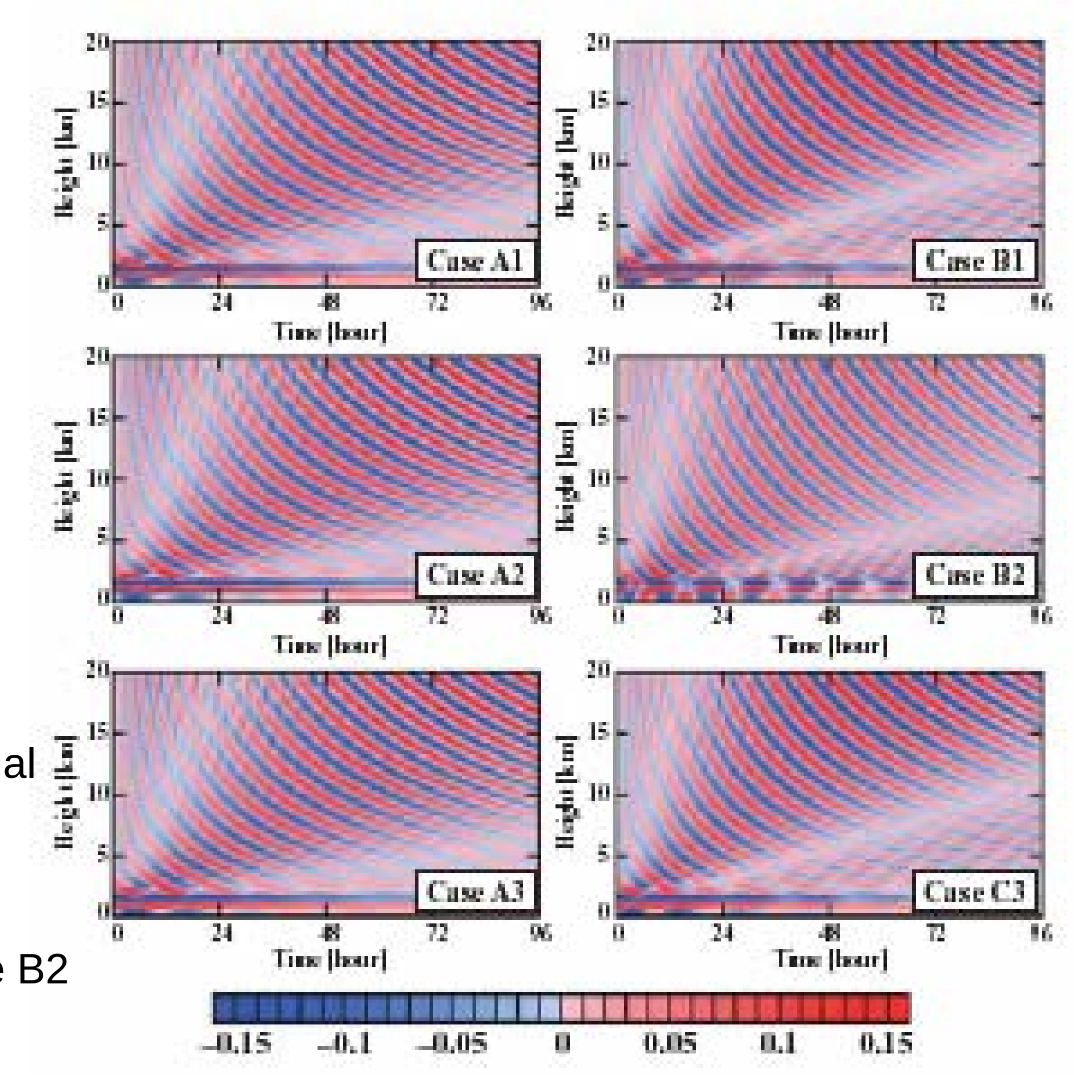

CIP-CSLR

- Conservative semi-Lagrangian scheme with rational function (Xiao et al. 2002) based CIP (Cubic-interpolated pseudopartcle, Yabe et al. 1991)
- Predict both the cell-integration and interface, like CIP for basic variable and its spatial gradient, which make it more accurate but increase little computation.
- Be conservative, oscillation-free, positive and no additional limiter needed.
- A high-accuracy scheme over merely one cell.

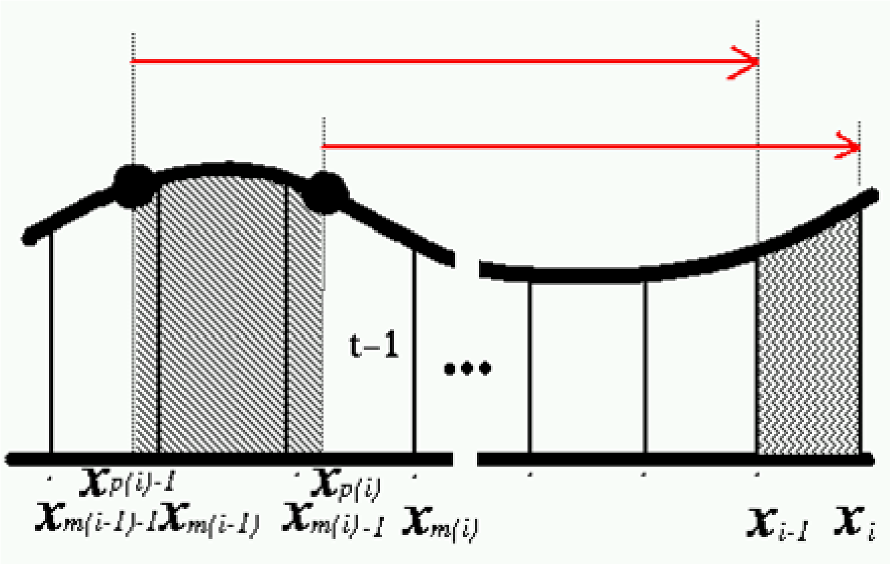

Results CFL=3

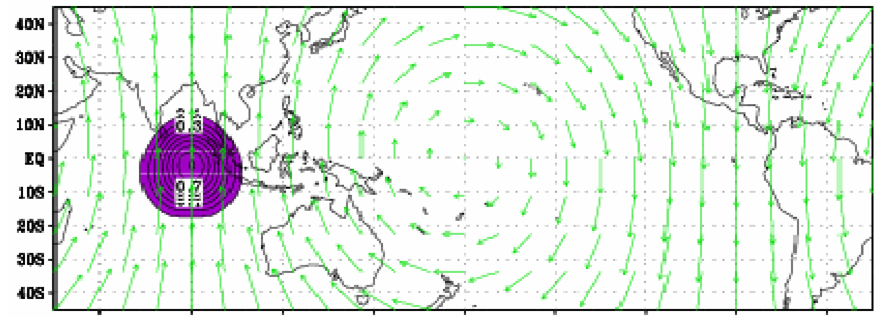

about 200km for horizontal

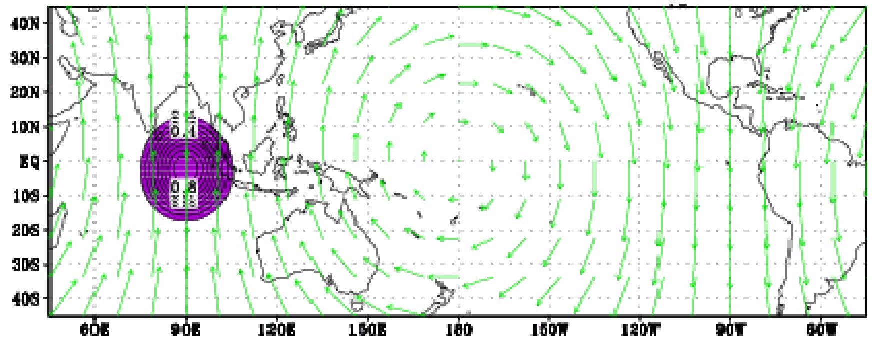

about 80km for horizontal

Implementation of Non-hydrostatic AGCM

		Non-hydrostatic AGCM	Non-hydrostatic OGCM
Equations System		Fully compressive N-S equations	non-hydrostatic･incompressive N-S equations
Grid System		Yin-Yang grid system	Yin-Yang grid system
Discrimination	Space	Arakawa-C grid(horizontal), z*(vertical)	Arakawa-C grid(horizontal), z(vertical)
	Time	4th order Runge-Kutta	4th order Runge-Kutta
Advection terms		5th order flux form, CIP-CSLR	5th order flux form
not Advection terms		4th order flux form	4th order flux form
Sound wave		HEVI, HIVI	Implicit methods(2-dimensional, 3-dimensional)
Gravity wave		-	
Microphysics		Qc, Qci, Qr, Qs, Qg	-
Cumulus Param.		Kain-Fritsch scheme	-
Turburance		Smagorinsky scheme (static), dynamic Smagorinsky[LES]	Smagorinsky scheme (static), dynamic Smagorinsky[LES]
		Nesting systems(1way,2way)	Nnesting systems(1way,2way)
			Tide, Multi-grid Methods(Poison eq.)
Parallelization		2-dim. decomposiotion, inter nodes:MPI, intra nodes:micro-task	2-dim. decomposiotion, inter nodes:MPI, intra nodes:micro-task

Preliminary Validation Condition

resolution	horizontal	11km, 5.5km,, 2.6km (regional:4.8km, 2.6km, 1.3km, 500m)
	vertical	32 layers(height: 30km)
prediction term		72 hours
initial time		00, 12UTC
initial data		observational global data distributed by JMA
side boundary		result data from global simulations
upper boundary		Rayleigh damping
bottom boundary		latest 1 day observational data before the time of simulation

Nested System

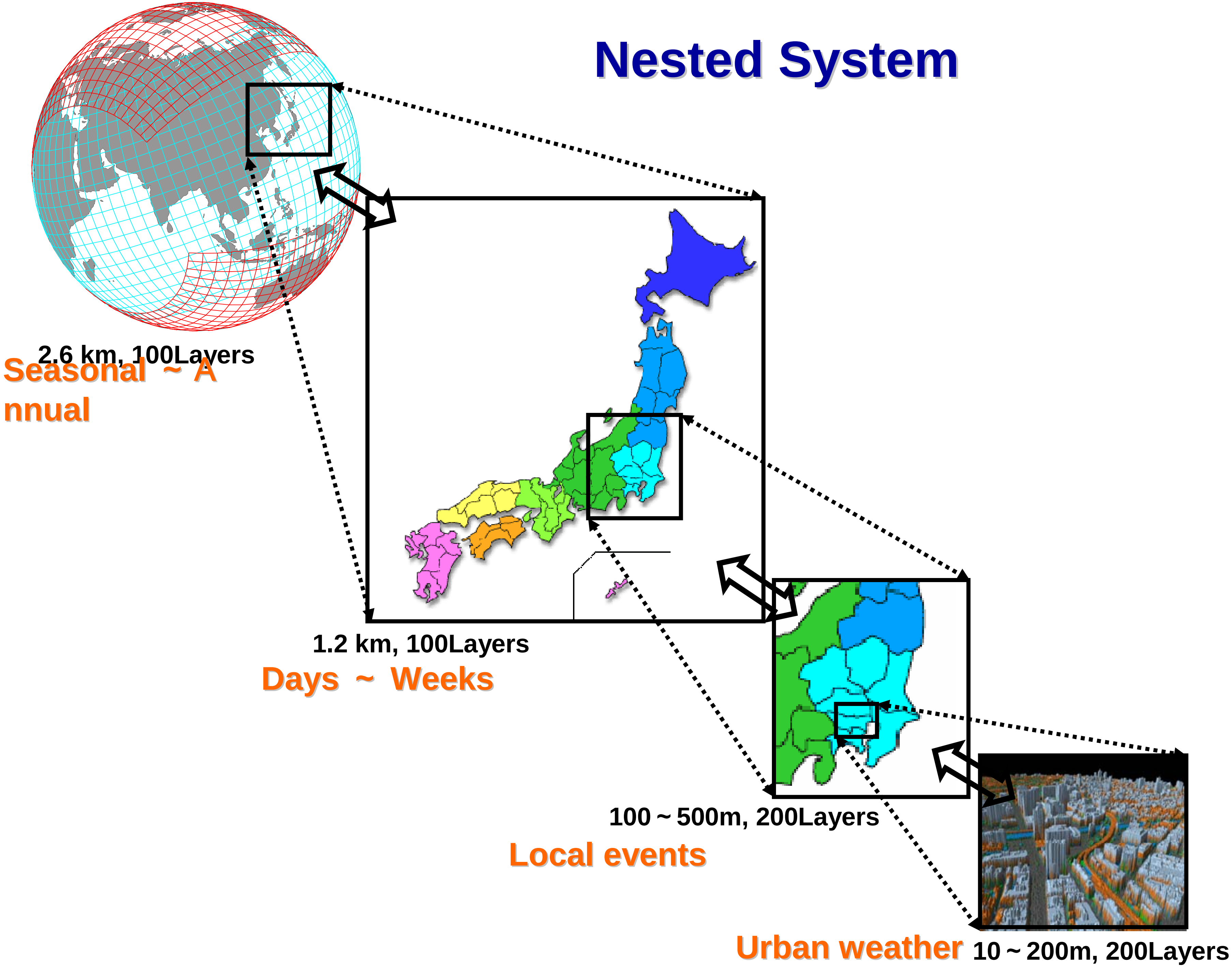

Preliminary Validation Results

Global，non-Hydrostatic, Cloud micro-physics

Typhoon during 7-11th August 2003

- **Tracked along Japan**
- **Heavy local rain in Kinki, Tokai, and Hokkaido regions**

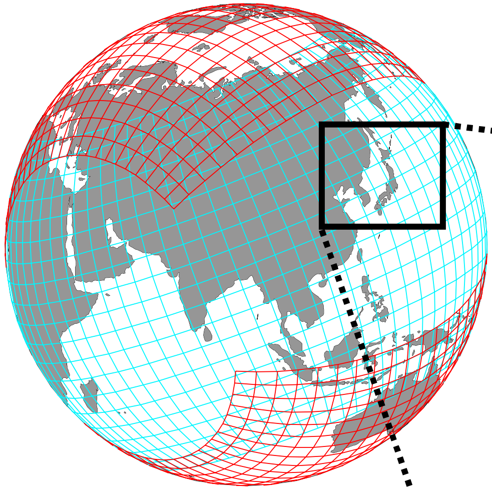

11 km, 32Layers

5.5 km, 32Layers

Global, SLP

Global, WSP

Japanese region., Precip., SLP

Japanese region,WSP

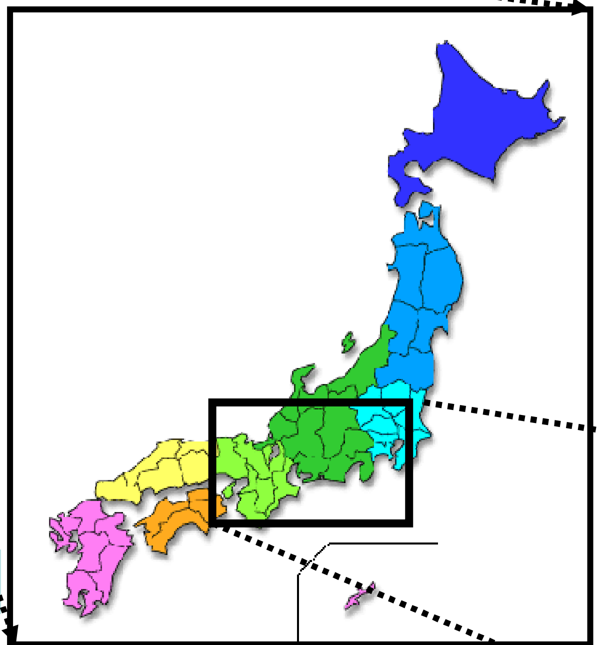

4.8 km, 32 Layers

Precip., SLP

WSP

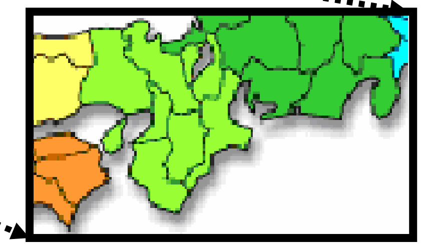

2.4 km, 32Layers

500m, 32Layers

Tracking of the Typhoon

Observation

平成15年8月　台風第10号に関する気象速報

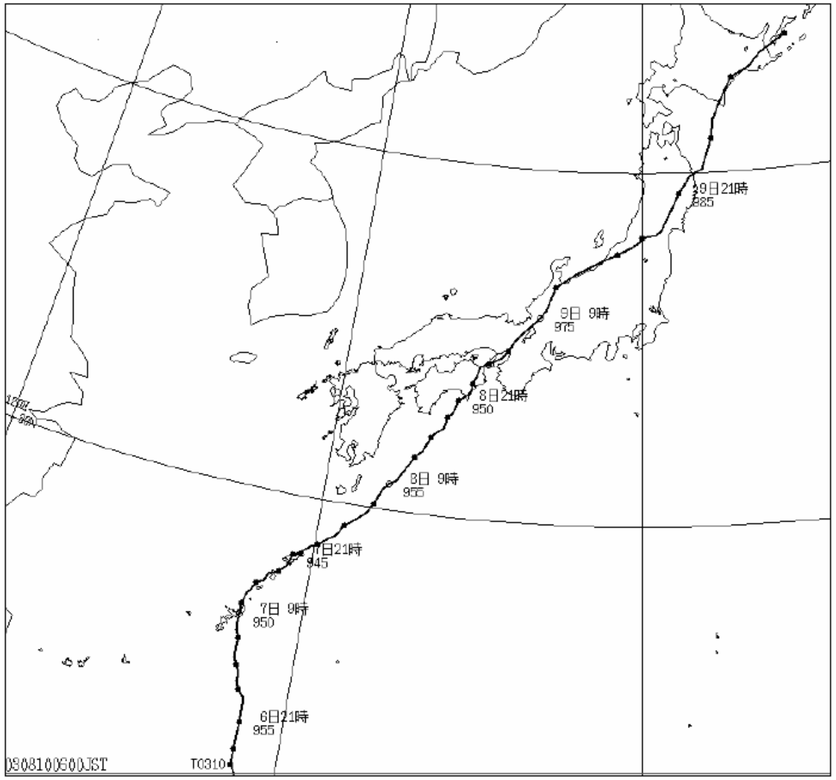

東　京

平成15年8月10日

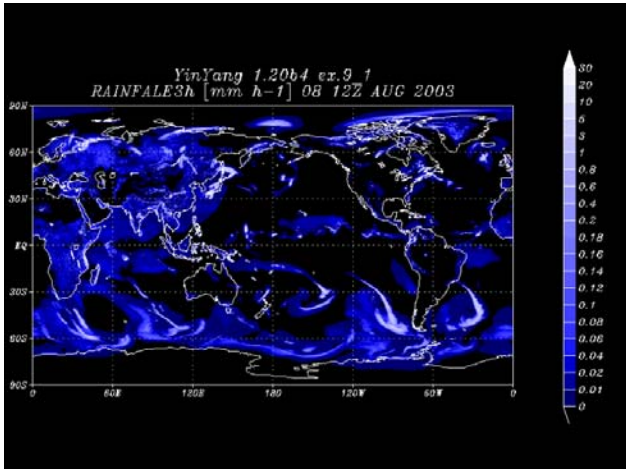
YinYang 1.20b4 ex.9_1
RAINFALE3h [mm h-1] 08 12Z AUG 2003

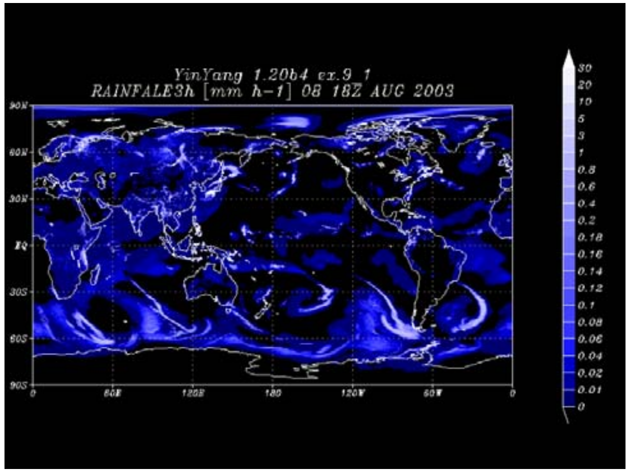
YinYang 1.20b4 ex.9_1
RAINFALE3h [mm h-1] 08 18Z AUG 2003

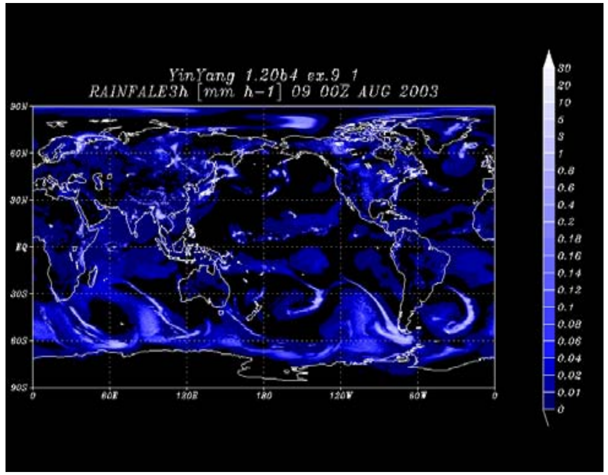
YinYang 1.20b4 ex.9_1
RAINFALE3h [mm h-1] 09 00Z AUG 2003

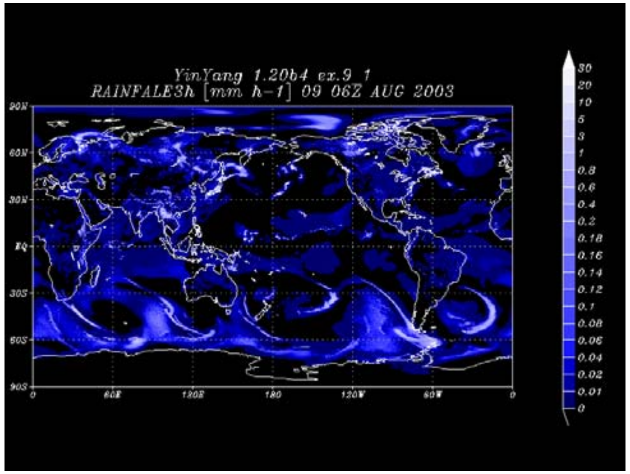
YinYang 1.20b4 ex.9_1
RAINFALE3h [mm h-1] 09 06Z AUG 2003

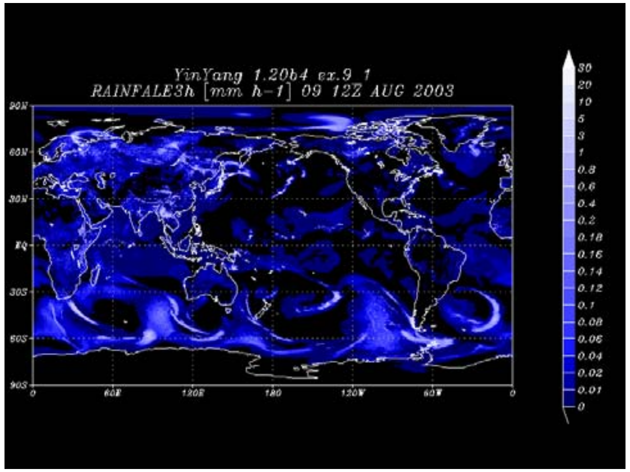
YinYang 1.20b4 ex.9_1
RAINFALE3h [mm h-1] 09 12Z AUG 2003

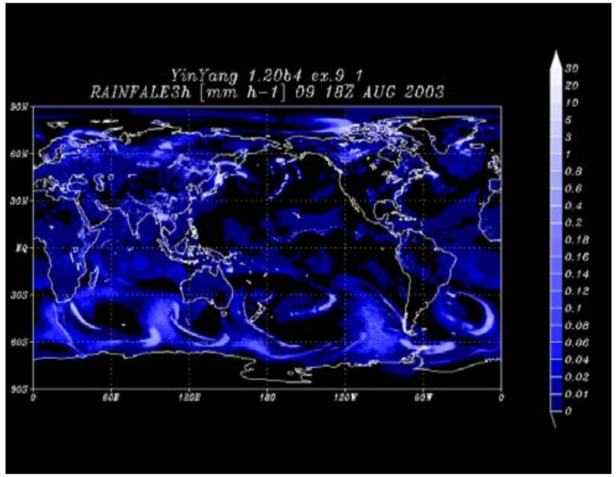
YinYang 1.20b4 ex.9_1
RAINFALE3h [mm h-1] 09 18Z AUG 2003

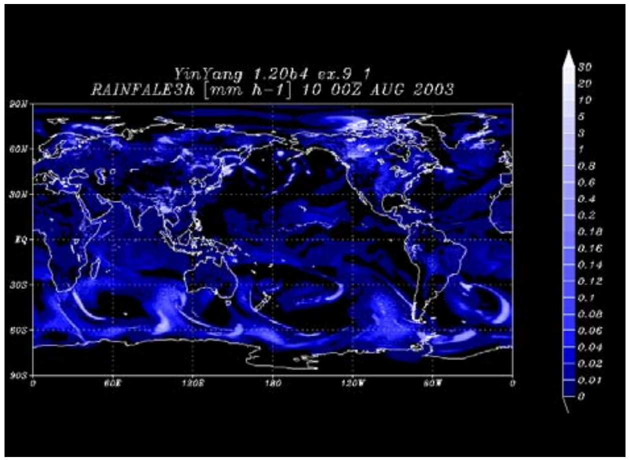
YinYang 1.20b4 ex.9_1
RAINFALE3h [mm h-1] 10 00Z AUG 2003

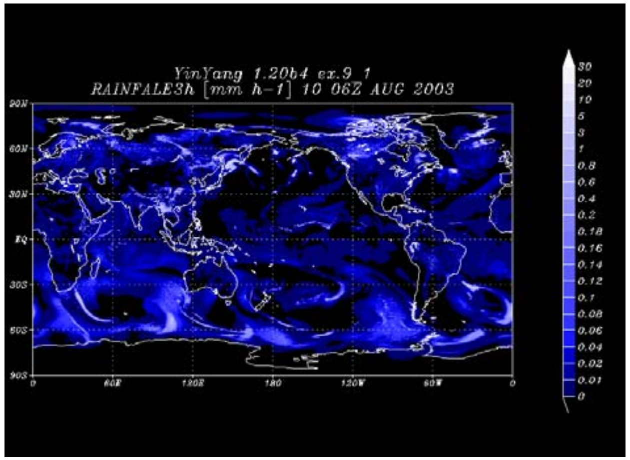
YinYang 1.20b4 ex.9_1
RAINFALE3h [mm h-1] 10 06Z AUG 2003

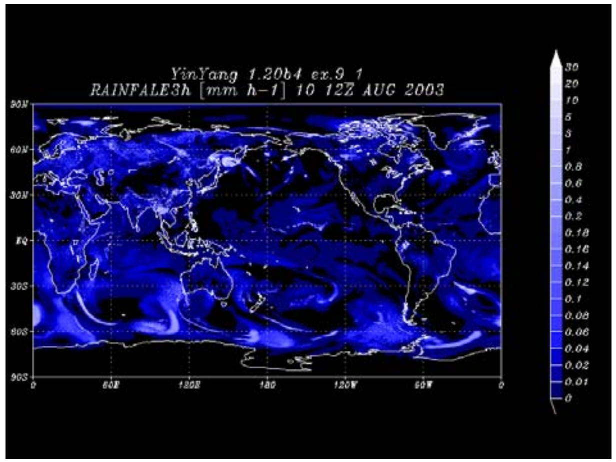
YinYang 1.20b4 ex.9_1
RAINFALE3h [mm h-1] 10 12Z AUG 2003

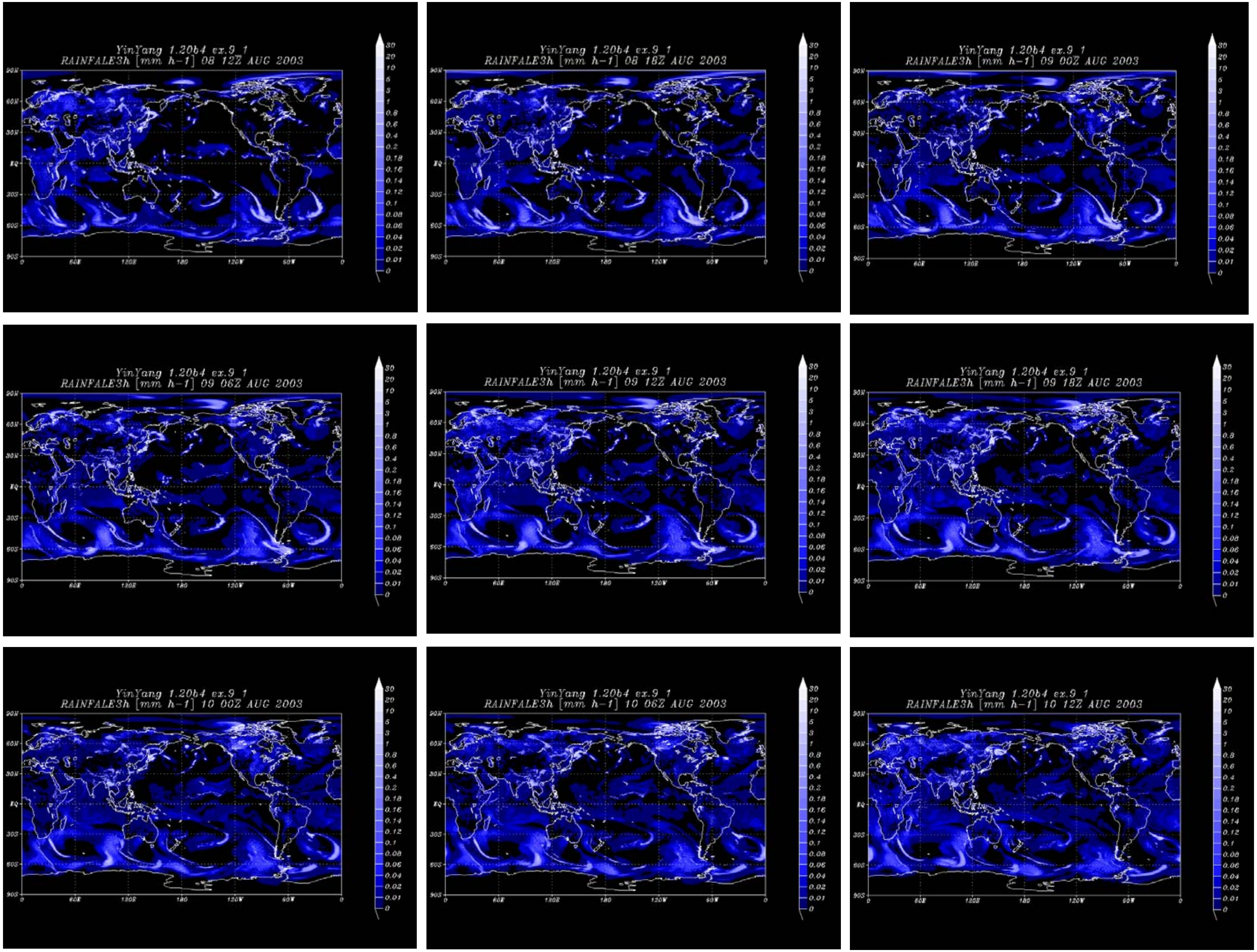
YinYang 1.20b4 ex.9_1
RAINFALE3h [mm h-1] 08 12Z AUG 2003
YinYang 1.20b4 ex.9_1
RAINFALE3h [mm h-1] 08 18Z AUG 2003
YinYang 1.20b4 ex.9_1
RAINFALE3h [mm h-1] 09 00Z AUG 2003
YinYang 1.20b4 ex.9_1
RAINFALE3h [mm h-1] 09 06Z AUG 2003
YinYang 1.20b4 ex.9_1
RAINFALE3h [mm h-1] 09 12Z AUG 2003
YinYang 1.20b4 ex.9_1
RAINFALE3h [mm h-1] 09 18Z AUG 2003
YinYang 1.20b4 ex.9_1
RAINFALE3h [mm h-1] 10 00Z AUG 2003
YinYang 1.20b4 ex.9_1
RAINFALE3h [mm h-1] 10 06Z AUG 2003
YinYang 1.20b4 ex.9_1
RAINFALE3h [mm h-1] 10 12Z AUG 2003

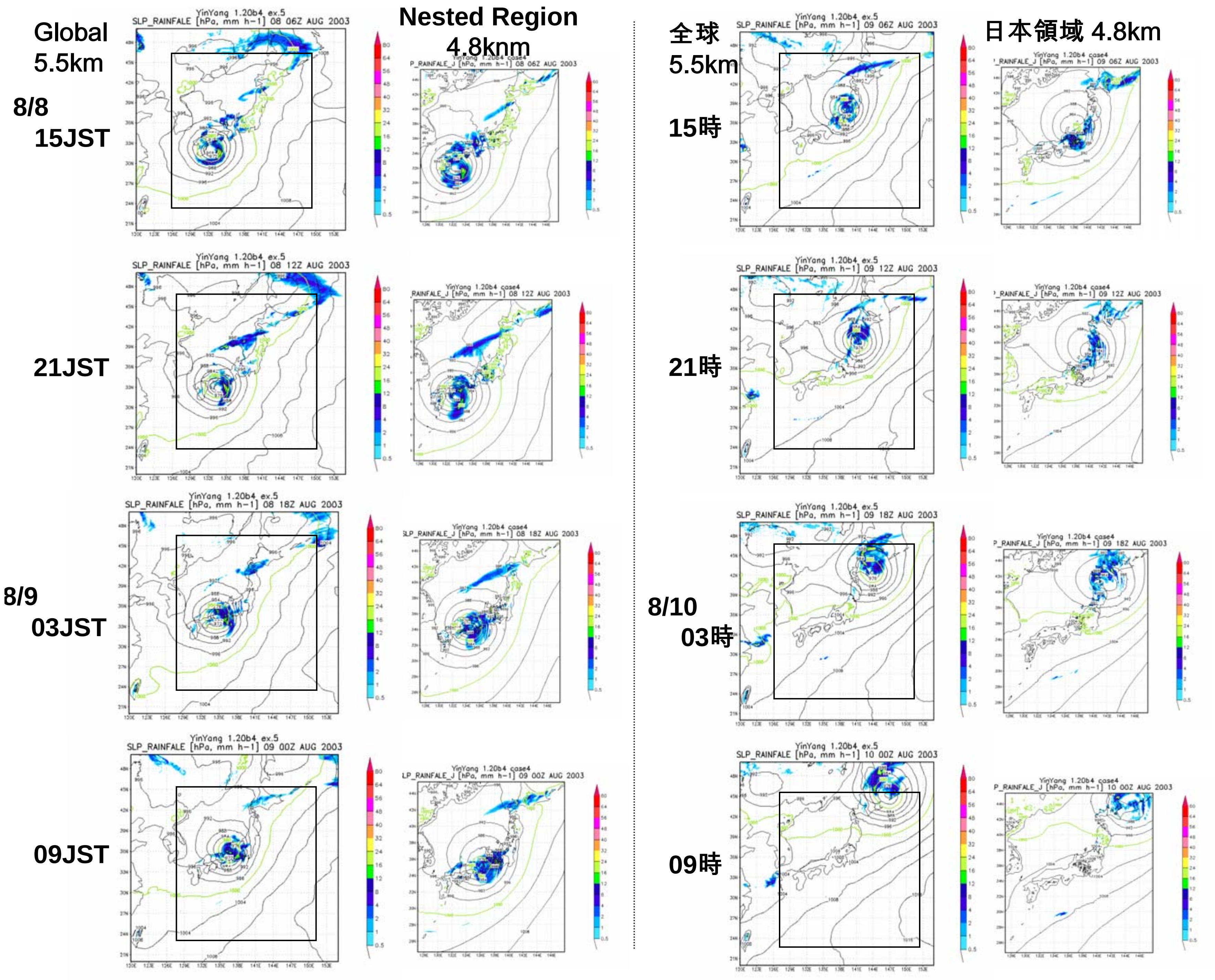

Global
5.5km
Nested Region
4.8knm
全球
5.5km
日本領域 4.8km
8/8
15JST
21JST
8/9
03JST
09JST
15時
21時
8/10
03時
09時
YinYang 1.20b4 ex.5
SLP_RAINFALE [hPa, mm h-1] 08 06Z AUG 2003
SLP_RAINFALE [hPa, mm h-1] 08 12Z AUG 2003
SLP_RAINFALE [hPa, mm h-1] 08 18Z AUG 2003
SLP_RAINFALE [hPa, mm h-1] 09 00Z AUG 2003
SLP_RAINFALE [hPa, mm h-1] 09 06Z AUG 2003
SLP_RAINFALE [hPa, mm h-1] 09 12Z AUG 2003
SLP_RAINFALE [hPa, mm h-1] 09 18Z AUG 2003
SLP_RAINFALE [hPa, mm h-1] 10 00Z AUG 2003
YinYang 1.20b4 case4

Precipitation

8/8 12JST | 15JST | 18JST | 21JST

2.4 km

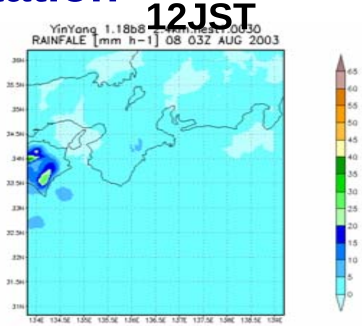

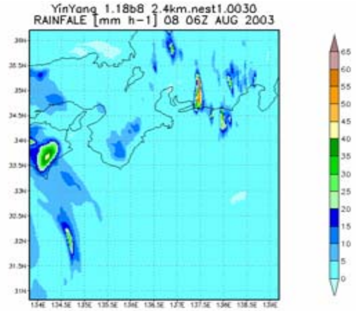

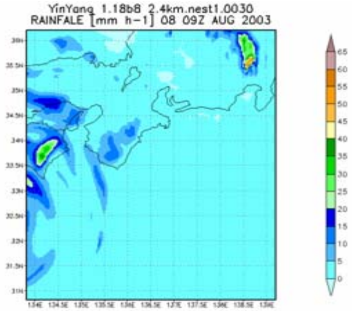

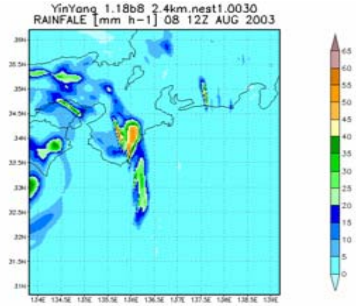

500m

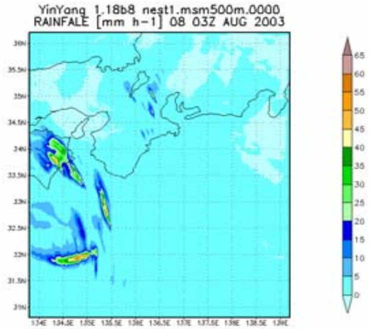

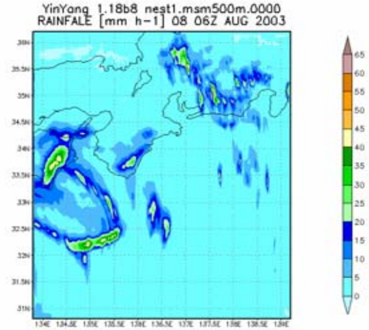

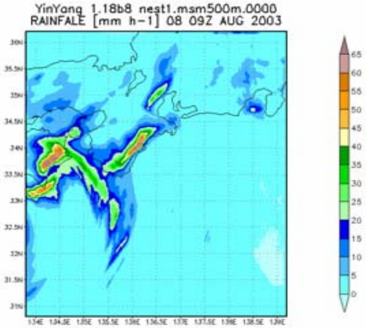

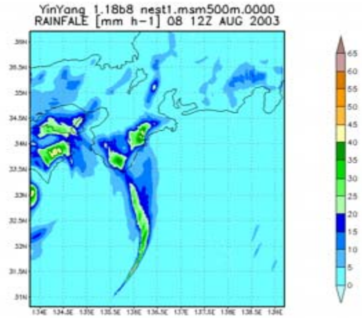

24JST | 8/9 03JST | 06JST | 09JST

2.4 km

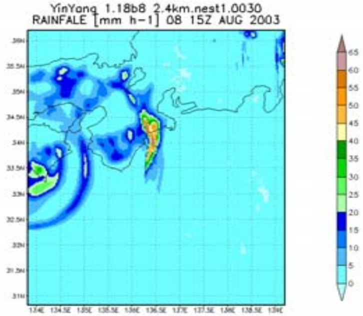

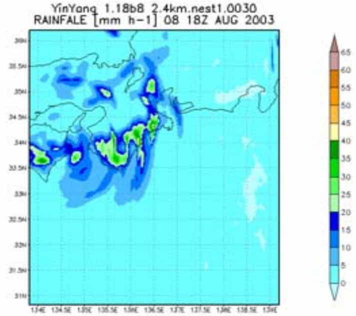

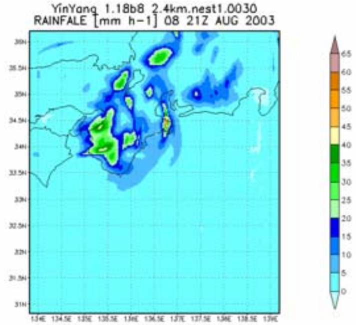

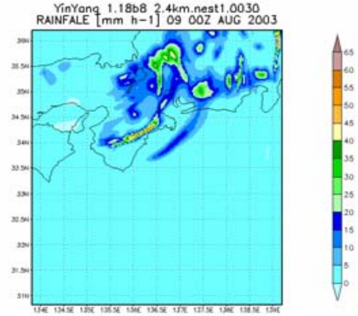

500m

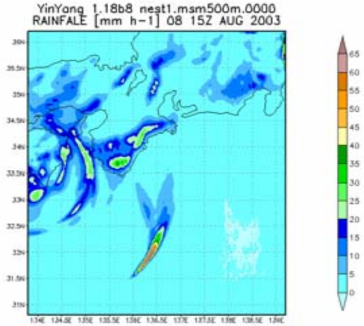

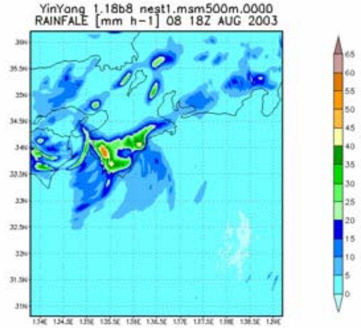

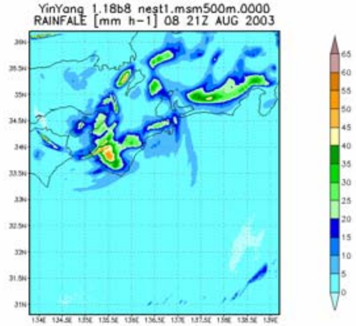

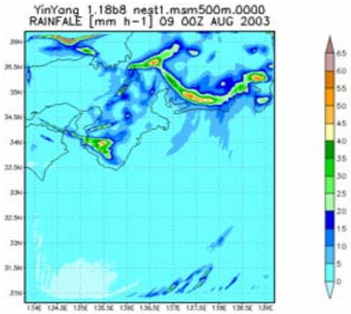

Tracking of Tyhoon: 7-10th August 2003

Observation

平成15年8月　台風第10号に関する気象速報

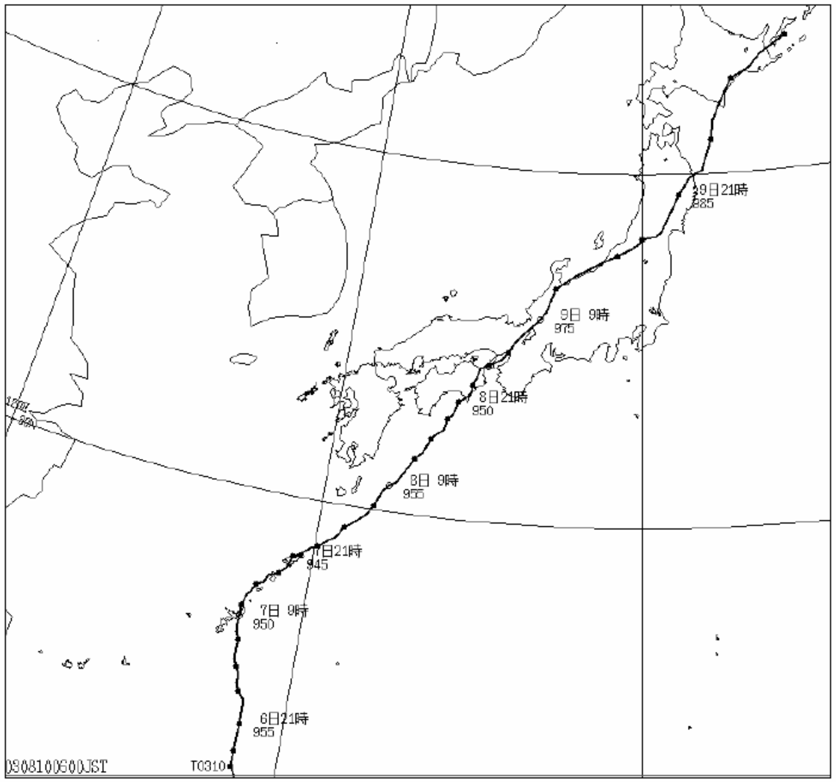

東　京　管　区　気　象　台

平成15年8月10日

Simulation results

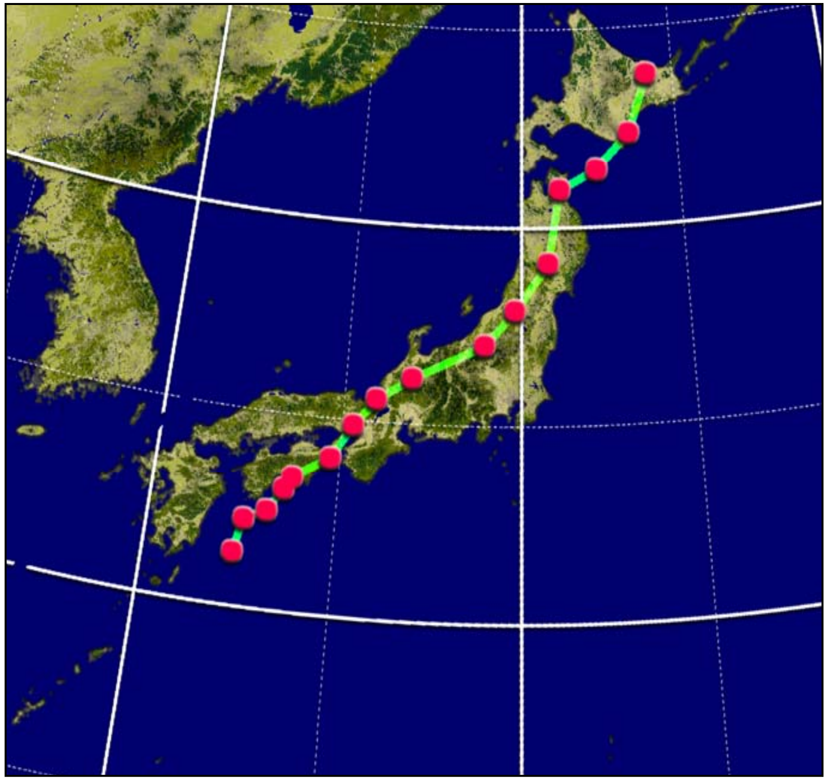

Communication cost imbalance on boundary regions

(a) Communication with 1-dimensional decomposition.

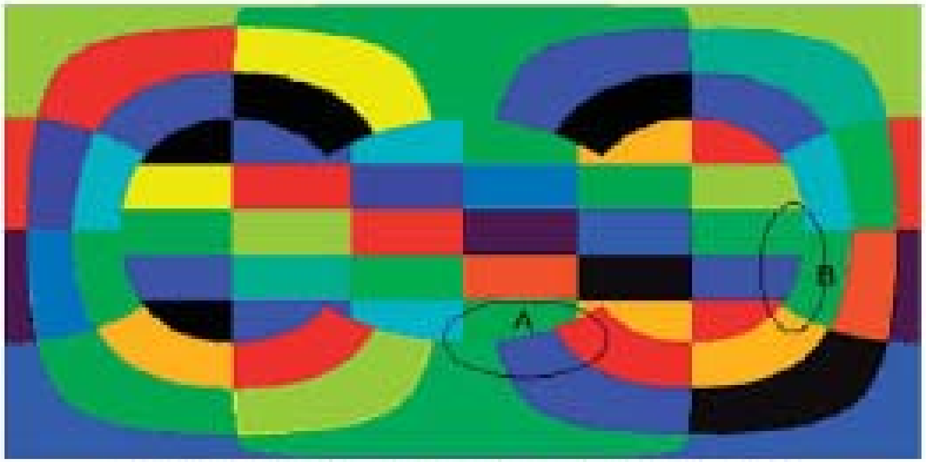

(b) Communication for two-dimensional distribution.

Perimeter of each colored region is corresponding to a mount of communication between processes.

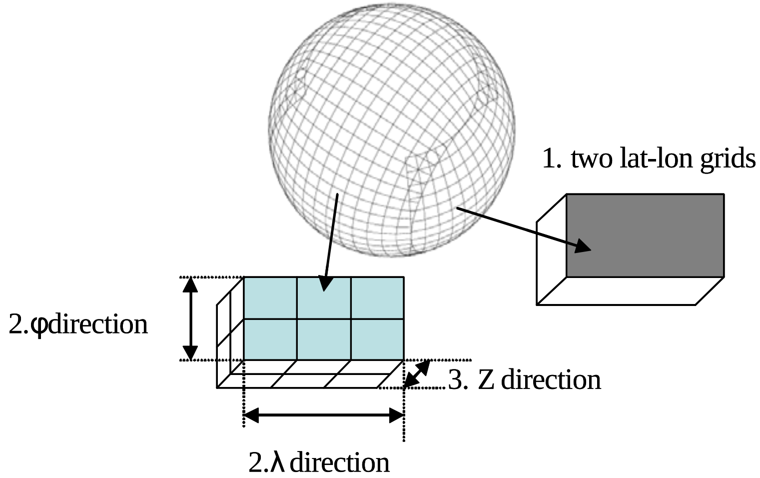

2 Dimensional Decomposition:

-Communication cost can be reduced.

-Computational cost imbalance between A and B regions can be avoided.

-For inter-node parallel processing, MPI library.

-Microtasking architecture was used for intra-node parallel processing.

Cost Performance of Dynamical Core on the Earth Simulator.

Performance statistics on the Earth Simulator.

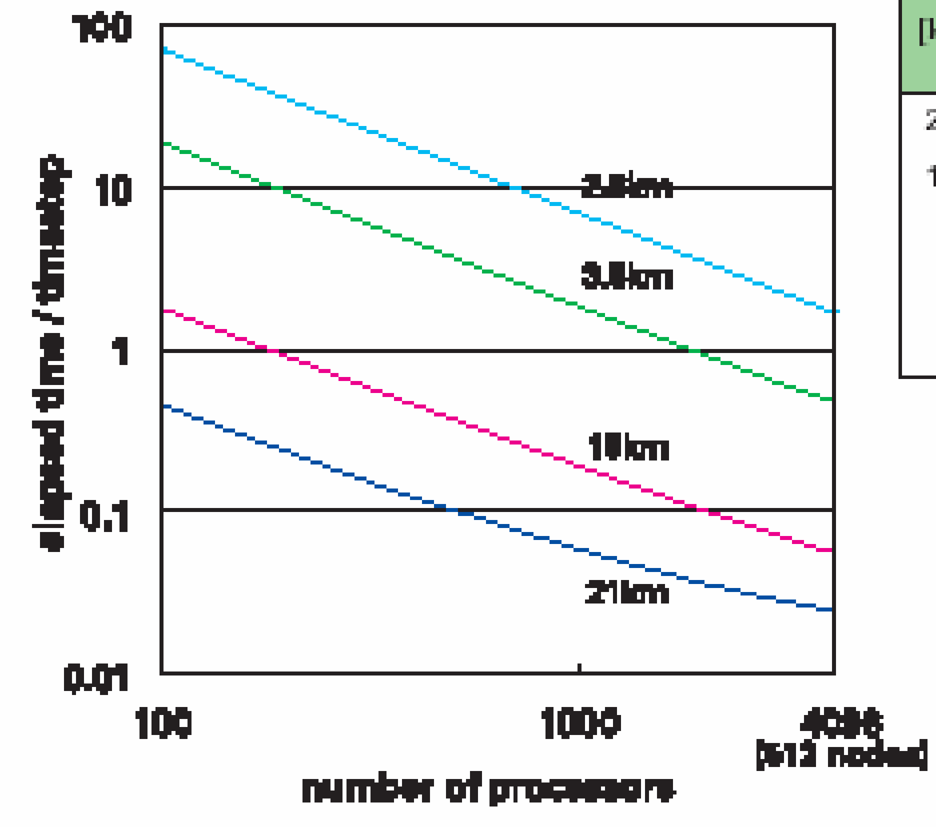

Current status of performance.

[km]	resolution grid points	#of nodes	peak ratio [%]	V.Op.Ratio [%]	VLEN
20.9	1440 x 480 x 96 x 2	6	58.1	99.53	236.8
10.4	2880 x 960 x 96 x 2	24	56.7	99.52	237.4
5.2	5760 x 1920 x 96 x 2	96	59.9	99.54	239.2
3.5	8640 x 2880 x 96 x 2	216	60.0	99.54	238.9
2.6	11520 x 3840 x 96 x 2	512	59.9	99.60	239.7

-Comparing the statistics between of AFES and our code with 10 km resolution for horizontal, our code is 10 times faster as CPU time Computational performance without CIP-CSLR

-2.6 km horizontal resolution has attained to about 60% of the theoretical peak performance 32.8 Tflops of 4096 processors (512 nodes).

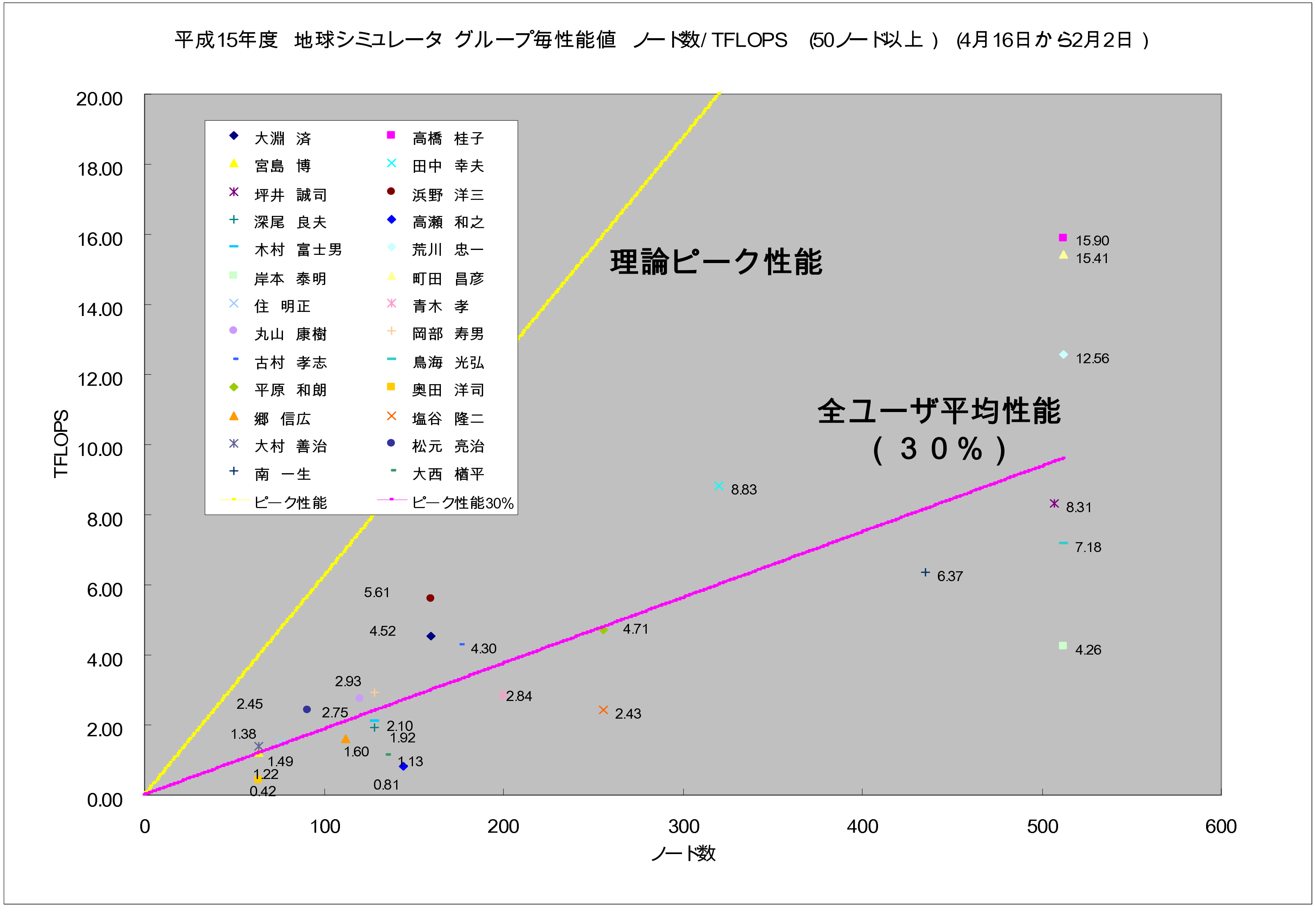

平成15年度　地球シミュレータ グループ毎性能値　ノード数/ TFLOPS　(50ノード以上）(4月16日から2月2日）
TFLOPS
ノード数
20.00
18.00
16.00
14.00
12.00
10.00
8.00
6.00
4.00
2.00
0.00
0
100
200
300
400
500
600
大淵　済
高橋　桂子
宮島　博
田中　幸夫
坪井　誠司
浜野　洋三
深尾　良夫
高瀬　和之
木村　富士男
荒川　忠一
岸本　泰明
町田　昌彦
住　明正
青木　孝
丸山　康樹
岡部　寿男
古村　孝志
鳥海　光弘
平原　和朗
奥田　洋司
郷　信広
塩谷　隆二
大村　善治
松元　亮治
南　一生
大西　楢平
ピーク性能
ピーク性能30%
理論ピーク性能
全ユーザ平均性能
（３０％）
15.90
15.41
12.56
8.83
8.31
7.18
6.37
5.61
4.52
4.30
4.71
4.26
2.93
2.84
2.45
2.75
2.43
2.10
1.92
1.38
1.49
1.60
1.13
1.22
0.42
0.81

Near Future Work

Just now kick off status to reproduce/predict non-hydrostatic phenomena such as typhoon, heavy rain in Baiu season, tornado and so on.

- Much more validation experiments for each of Atmosphere and Ocean components.

- Cost tuning with CIP-CSLR

- Experiments by using regional coupled simulation code with ultra high resolution.

- Preliminary experiments with non-hydrostatic coupled code have stated in autumn of 2004.